Marine and Petroleum Geology 59 (2015) 406–428

Contents lists available at ScienceDirect

Marine and Petroleum Geology

journal homepage: www.elsevier.com/locate/marpetgeo

Research paper

Repeat ridge jumps and microcontinent separation: insights from NE Arabian Sea

Achyuta Ayan Misra [a, b], Neeraj Sinha [a], Soumyajit Mukherjee [b, *]

[a] Petroleum Exploration, Reliance Industries Ltd., Navi Mumbai 400 701, Maharashtra, India
[b] Department of Earth Sciences, Indian Institute of Technology Bombay, Powai, Mumbai 400 076, Maharashtra, India

ARTICLE INFO

Article history:
Received 14 November 2013
Received in revised form
31 May 2014
Accepted 26 August 2014
Available online 18 September 2014

Keywords:
Ridge jump
Seychelles–India separation
Laxmi ridge
Gravity modelling
Volcano-stratigraphy

ABSTRACT

Microcontinents separate due to ridge jumps associate either asymmetric sea floor spreading or plume–ridge interactions. India separated from Seychelles at ~64 Ma by asymmetric sea floor spreading initially when the spreading centre in the Mascarene Basin jumped towards the Indian sub-continent between magnetic chrons C29 and C28. The subsequent tectonics is difficult to comprehend since Laxmi Ridge-another microcontinent-formed during the later phase. Most of the studies considered the Laxmi Ridge as a sliver. Others considered it to be oceanic crust. High resolution, deep (~25 km) seismic data reveals that (*i*) the ridge possesses > 15 km deep sea-ward dipping reflector (SDR) packages; (*ii*) normal faulted rift valleys devoid of syn-rift sedimentary packages; and (*iii*) axial magma chambers 5–7 km beneath the ridge top. Additionally, from 2D forward gravity models we deduce that the ridge most possibly comprises of high density (oceanic) crust. We conclude the Laxmi Ridge to be indeed composed of oceanic crust and a fossil spreading centre. We thus identified the ridge jumps and their relation to the Seychelles microcontinent separation.

Previous numerical models suggest that the time required for a ridge jump is controlled by magmatic heating, spreading rate at the ridge, and plate ages. For repeated ridge jumps, the additional factor is the dynamic relation between the plume and lithosphere in terms of melt transfer and heating. We find that the medium spreading rates and high magmatic heating due to the Réunion plume and young plates favoured rapid and repeated ridge jumps towards the plume.

1. Introduction

Microcontinents or continental slivers (Müller et al., 2001; Péron-Pinvidic and Manatschal, 2010) develop commonly during continental breakup as either emergent e.g. Seychelles- or Jan Mayen Microcontinent (see Rey et al., 2003; Scott et al., 2005; Péron-Pinvidic et al., 2010) or buried e.g. Elan Bank (see Borissova et al., 2003) masses of continental crust 'floating' on oceanic lithosphere. The Seychelles is one of the best examples of a microcontinent since it has Precambrian granitic outcrops and is surrounded by oceanic crust (Schlüter, 2006; Hammond et al., 2013). Their genesis is attributed to two processes: *(i)* plume-assisted ridge propagations/jumps (Mittelstaedt et al., 2008, 2011); and *(ii)* spreading asymmetries at mid-oceanic ridges and resulting ridge reorganizations (Goff and Cochran, 1996). The Seychelles microcontinent separated from India at ~64–62 Ma (Collier et al., 2008) with prolific volcanism affecting India and Seychelles during Late Cretaceous to Early Paleocene (Chenet et al., 2007; references therein; Owen-Smith et al., 2013), popularly known as Deccan Traps for the onland volcanics (Mahoney, 1988) (Fig. 1). The track of the Réunion plume, related to the Seychelles-India separation, is demarcated by the Chagos-Maldive-Laccadive Ridge up to the Central Indian Ridge (CIR, Fig. 1; Duncan, 1990; Biswas, 2014). The Chagos-Maldive-Laccadive Ridge crossed the CIR to form the Saya de Malha bank (Fig. 1)- a sea mound with unconfirmed crustal nature (Eagles and Wibisono, 2013). The Chagos-Maldive-Laccadive Ridge might have continental fragments broken off during India-Madagascar separation (Nair et al., 2013; Torsvik et al., 2013). The NW-SE segment of the CIR is known as Carlsberg Ridge (Fig. 1). Thus, a combination of the rifting and volcanism formed one of the largest and most elegant magma-rich rifted passive margins. Magma-rich/magmatic/volcanic passive margins (Levell et al., 2010; Manatschal and Karner, 2012), as

* Corresponding author.
E-mail addresses: soumyajitm@gmail.com, smukherjee@iitb.ac.in (S. Mukherjee).

http://dx.doi.org/10.1016/j.marpetgeo.2014.08.019
0264-8172/

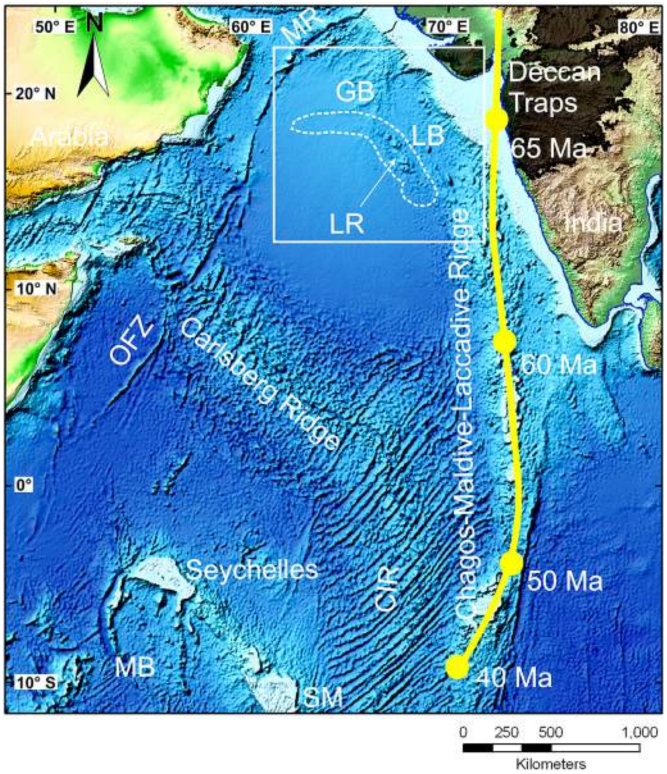

Figure 1. Map of the study area, within white rectangle. Adjoining areas with hill shaded bathymetry and topography. Areal extent of the Deccan Traps is shown in dark grey in the N part of the W continental margin of India. White dotted line: extent of the Laxmi Ridge. MR = Murray Ridge, LR = Laxmi Ridge, LB = Laxmi Basin, GB = Gop Basin, OFZ = Owen Fracture Zone, SM = Saya de Malha bank; MB = Mascarene Basin, CIR = Central Indian Ridge. Thick solid line: track of the Réunion hotspot (from Duncan, 1990). Bathymetry data: from Sandwell and Smith (2009); topography data: from Becker et al. (2009). This topography and bathymetry data, in a similar colour scheme, is used by other authors (e.g. Eagles and Wibisono, 2013) and thus this map may seem identical to those. Modified from fig. 1 of Misra et al. (2014).

opposed to magma-poor/amagmatic/non-volcanic margins (Manatschal, 2004; Whitmarsh and Manatschal, 2012), are characterised by relatively high volume of syn-rift volcanics and are associated commonly with mantle plumes (Menzies et al., 2002; Franke, 2013; Misra and Mukherjee, in preparation). Plumes are relevant in "active" rifting at magma-rich margins (Courtillot et al., 1999; Müller et al., 2001). India-Seychelles rifted from Madagascar by spreading the sea floor asymmetrically in the Mascarene Basin till chron C27 (Bernard and Munschy, 2000; Müller et al., 2001). This led a ridge jump towards the Réunion hotspot (Dyment, 1998). The magnetic anomalies indicate the ridge jump at chron C28 (63.4 Ma) (Collier et al., 2008). See figure 16.5 of Arora et al. (2003) for magnetization distribution map of Indian continent and surrounding region. Mahadevan (1994) reviewed gravity magnetic and seismic findings of our present study area. Rifting between Seychelles and India generated an "enigmatic" feature: the Laxmi Ridge (Todal and Edholm, 1998) (Fig. 2). This ~100 km wide and complex ridge is ~ E–W elevated basement at N from 63 to 66° longitude and ~ NW-SE at S from 19 to 14° N latitude (review: Prodehl and Mooney, 2012; also see Valdiya, 2010). Figure 2 shows the possible extent of the Laxmi Ridge mapped from free air gravity anomaly data, as in previous studies. The petroleum producing giant "Bombay High" ('BH' in Fig. 2) and other fields are located E to the study area (see Biswas, 2012). The Laxmi Ridge is a gravity low skirted by gravity highs. A sharp change in gravity of ~ 60 mGals defines the boundary.

The plume-ridge interaction and ridge jumps within chron C28–C26 has neither been studied well (e.g. Minshull et al., 2008) nor is straightforward. This is because previous workers considered the Laxmi Ridge to be a continental sliver (Naini and Talwani, 1982; Bhattacharya et al., 1994; Talwani and Reif, 1998; Todal and Edholm, 1998; Krishna et al., 2006; Collier et al., 2008) based on gravity inversion modelling, shallow seismic data, and seismic refraction lines and points.

This study, entirely in the submarine realm of the Indian plate (Fig. 1), re-examines the Laxmi Ridge with vintage single channel seismic lines (from Lamont-Doherty through GeoMapApp; http://www.geomapapp.org) and high resolution reflection seismic lines of long (18 s) record length (from ion-GX Technology), seismic refraction points data (from Naini and Talwani, 1982), reinterpretation of the gravity- (Sandwell and Smith, 2009) and magnetic anomaly data (Maus et al., 2007) constrained with the reflection seismic data, seismic volcano-stratigraphy and well data to unravel its crustal structure. We interpret seismic facies on the seismic sections to understand the geology of the region and corroborate with the geophysical constraints (gravity, compressional wave velocity and magnetic). Did plume-assisted ridge jumps separate the Seychelles microcontinent? Or, did severing happen by asymmetric spreading in the NE Arabian Sea, after the ridge jump from the Mascarene Basin? We infer the crustal nature of the Laxmi Ridge from seismic and gravity data and interpret the magnetic data to study the chronology of the ridge jumps related to the Seychelles microcontinent separation. Understanding tectonics of the study area is important in hydrocarbon exploration (e.g. Biswas, 1989; Vaidyanadhan and Ramakrishnan, 2008).

2. Regional context

2.1. Tectonic elements

The important aseismic ridges in the Arabian Sea are the Laxmi-, Comorin-, Chagos-Maldive-Laccadive ridges. The Carlsberg- and the Central Indian Ridges are active spreading centres; the Owen Fracture Zone is a > 3000 km long ~ NNE trending fracture zone separating the Indian- and Arabian plates (Fig. 1; Kearey et al., 2009). The Owen Fracture Zone continues NE as the Murray Ridge. The Murray Ridge is considered as a Mesozoic oceanic block deformed under transpression by the sinistral Owen Fracture Zone during Early Paleocene and by transtension during Oligo-Miocene (Corfield et al., 2010). The Laxmi Ridge, an important tectonic element, is located W to the western continental sheared margin of India. Sheared or oblique continental passive margins, as opposed to orthogonal ones, are those where the net extension is not perpendicular to the margin (e.g. Green, 2011; Baudot et al., 2013). Evidences of shearing in the margin have been reported from onland and offshore studies around Mumbai (shelf) region (Ghosh and Zutshi, 1989; Misra et al., 2014). S to the present study area, the Konkan-Kerala margin formed by oblique rifting of Madagascar from India (Subrahmanyam and Chand, 2006; Reeves, 2013, 2014). The Laxmi Ridge (Fig. 2) divides the northern Arabian Sea into Western-and Eastern Basins (Naini and Talwani, 1982; reviews by Bastia and Radhakrishna, 2011). The Western Basin starts from the S/SW edge of the ridge and continues up to the present day Carlsberg Ridge (Krishna et al., 2006). The Laxmi Basin (LB in Fig. 1) represents the region between the ~ NW-SE segment of the Laxmi Ridge and the Indian subcontinent. There are isolated highs named Wadia Guyot, Panikkar and Raman- Seamounts (Karlapati, 2004; Krishna et al., 2006; Bhattacharyya et al., 2009). On the other hand, the Gop Basin (GB in Fig. 1) lies between the ~ E–W segment of the Laxmi Ridge and the Indian sub-continent. The Eastern Basin,

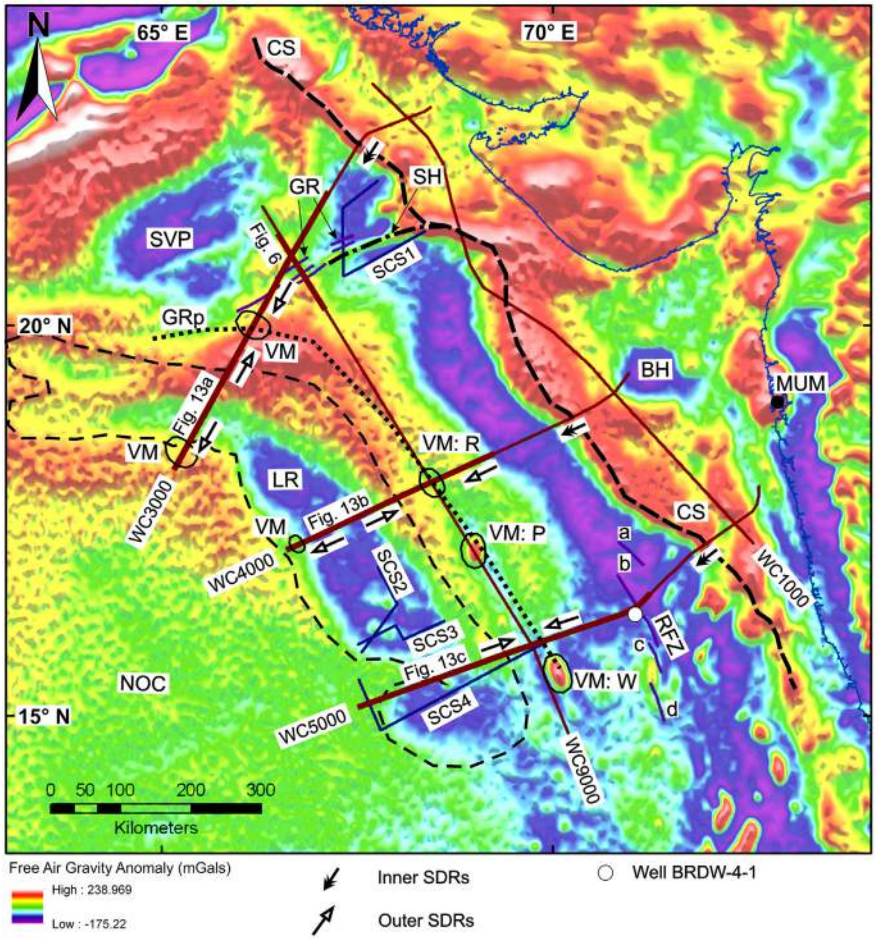

Figure 2. The study area showing the seismic sections we studied overlaid on hill-shaded free-air gravity anomaly data. Thin lines with 'WC' prefixes: ion-GXT lines used for the seismic interpretation (with line numbers); Thick lines with 'WC' prefixes: lines used for 2D forward gravity model in Figures 13, 14. Lines with 'SCS' prefixes: vintage single channel seismic (SCS) lines. Black dashed outline: extent of the Laxmi Ridge (labelled LR), mapped from seismic sections and gravity anomaly data. Thick black dashed line labelled CS: continental shelf, black dotted line (labelled GRp) marks Gop Rift as per the prior understanding. GR = Gop Rift faults as mapped from seismic; RFZ = Ratnagiri Fracture Zone; SVP = Saurashtra Volcanic Platform; SH = Saurashtra High (black dash dot line); VM = Volcanic mound mapped from gravity and/or seismic data, (see Figs. 8,9); W: Wadia Guyot; P: Panikkar Seamount; R: Raman Seamount; BH: Bombay High field, NOC = "Normal" oceanic crust, MUM: Mumbai city (Bombay = Mumbai). Arrows: Inclination directions of Seaward Dipping Reflector (SDR) complexes, different arrows for Inner and Outer SDRs. See sub-section 3.1 for details of the gravity data used.

comprising of the Laxmi- and the Gop Basins, thus lies between the Laxmi Ridge and the Indian sub-continent (Naini and Talwani, 1982). The Gop Basin/Rift/Palitana Ridge (Yatheesh et al., 2009), a part of the Gop/Laxmi Basin (Figs. 1 and 2), is an aborted oceanic spreading centre that initially broke Seychelles from India (Bhattacharya et al., 1994; Yatheesh et al., 2009; review: Mukhopadhyay et al., 2008; Dyment et al., 2012; Yatheesh et al., 2013). Seismic sections reveal that the basements of the Laxmi Basin and the Laxmi Ridge are undulated (e.g. figs. 3, 4 of Krishna et al., 2006, figs. 3, 6 of Corfield et al., 2010, fig. 7 of Calvès et al., 2011). In contrast, the basement of the Western Basin is rather flat (Krishna et al., 2006). This Western Basin comprises of ~8 km thick 'normal' oceanic crust (Todal and Edholm, 1998). The Indian plate is delimited by the Owen Fracture Zone-Murray Ridge in the W and Carlsberg Ridge in the SW. These lie W and SW, respectively, to the present study area (Fig. 1).

Heat flow measurements are available in the study area (Anderson et al., 1977) and N of it from seismic Bottom Simulating Reflectors (BSRs) and well data (Calvès et al., 2010). Heat flow on the Laxmi Ridge and Laxmi Basin range 50–60 mW m^{-2}. This matches well with the global averages heat flow of ~60 mW m^{-2} for 60–65 Ma old oceanic crust (McKenzie, 1978; Stein and Stein, 1992; see also pp. 130 of Kearey et al., 2009; and fig. 1b of Calvès et al., 2010).

2.2. Implications of gravity & seismic velocities

The Laxmi Ridge was interpreted as thinned continental crust, i.e. continental sliver/microcontinent based mainly on 2D gravity inversion models and seismic velocity structures (Naini and Talwani, 1982; Bhattacharya et al., 1994; Talwani and Reif, 1998; Todal and Edholm, 1998; Krishna et al., 2006; Collier et al., 2008). The Laxmi Ridge shows a negative Airy (T = 30 km) isostatic anomaly (Naini and Talwani, 1982). Further, density profiles constructed by inverting the gravity anomaly data show the Laxmi Ridge to be composed either of continental- (Talwani and Reif, 1998; Todal and Edholm, 1998 Radha Krishna et al., 2002; Krishna et al., 2006; Ajay et al., 2010) or oceanic crust (Pandey et al., 1995; Singh, 1999; Rajaram et al., 2011). Few workers doubted the continental crust interpretation of the Laxmi Ridge (e.g. see fig. 2b of Minshull et al., 2008 and fig. 3 of Calvès et al., 2011), mentioning that it can be either continental or oceanic (Minshull et al., 2008). Mishra (2012) reviewed gravity data for Laxmi ridge and adjoining regions.

Seismic refraction points (Naini and Talwani, 1982) reveal a three-layered crustal of the Laxmi Ridge with 5.43–7.15 km s^{-1} of P-wave velocities. The Mohorovičić discontinuity (Moho) was not imaged in the Eastern Basin. However, an extrapolated velocity

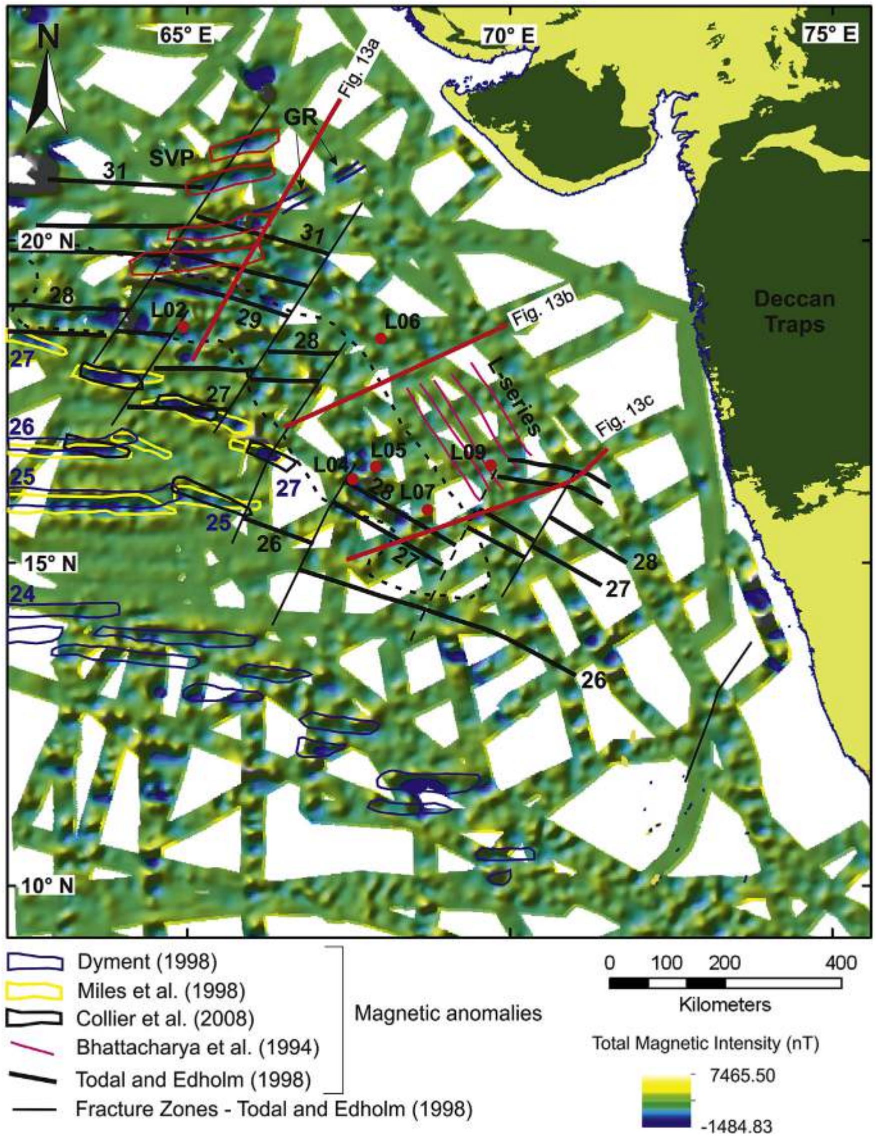

Figure 3. Total magnetic intensity map (data from National Geophysical Data Center), 30–100 km band pass, with magnetic seafloor spreading anomalies interpreted by previous authors (mentioned in the legend). Numbers in bold are magnetic chrons interpreted other authors (27 = C27, 26 = C26 etc.). GR: Gop Rift; Solid bold polygons near GR: magnetic anomalies mapped in this study. See sub-section 3.2 for details. Deccan basalts and all other lithologies are represented in two different colours. This diagram is plot of Collier et al.'s (2008) data on their map. Modified from fig. 19 of Misra et al. (2014). Note that Collier et al. (2008) presented earlier authors' data in a map. And Misra et al.'s (2014) fig. 19 plotted Collier et al.'s (2008) data on their map. See sub-section 3.2 for details of the magnetic data used. (For interpretation of the references to colour in this figure legend, the reader is referred to the web version of this article.)

indicated possibly a ~17 km deep Moho at the Eastern Basin and ~21 km beneath the Laxmi Ridge (Naini and Talwani, 1982). Citing P-wave velocities of ~6.2 km s^{-1} at the Laxmi Ridge (middle crust layer) against ~ 6.6 km s^{-1} in the Western Basin, the Laxmi Ridge was proposed to be granitic (Krishna et al., 2006). There is one refraction line in the region (Minshull et al., 2008). It trends ~ N–S and lies towards the western end of the E–W segment of the Laxmi Ridge (close to and W of 65° longitude). Records of seismic waves crossing deep crust were unavailable. Thus, the Moho was not deciphered conclusively beneath the Laxmi Ridge. Interpreting seismic refraction velocities, the Laxmi Ridge can either be composed of thinned, highly intruded continental crust or a pre-existing oceanic crust (Minshull et al., 2008; review: Bhattacharya and Chaubey, 2001). The velocity structure of the Laxmi Ridge corresponds with oceanic plateaus from other parts of the world-such as the North Atlantic margins, the Icelandic oceanic crust and the thickened oceanic crust of East Greenland (Calvès et al., 2011). The high velocity lowermost layers of the Laxmi Ridge and the Laxmi Basin were interpreted in terms of magmatic underplating (Pandey et al., 1995; Miles et al., 1998; Singh and Mall, 1998; Radha Krishna et al., 2002; Singh, 2002; Minshull et al., 2008; Rajaram et al., 2011). Such high velocity underplating was found beneath the Laxmi Ridge, Western continental margin of India, and at the Seychelles bank (Armitage et al., 2011). Thus, this is a possible result of the Réunion plume below the Indian plate and Seychelles microplate before or during rifting. Also, the seismic velocity indicates an extended oceanic crust velocity structure on the Laxmi Ridge (Todal and Edholm, 1998; their fig. 9). The seismic velocities and magnetic interpretation cannot discriminate the crustal nature of Laxmi Ridge (Minshull et al., 2008).

Reflection seismic sections suggest the presence of ~100 km long volcanic platform S of the Indus delta, named as the

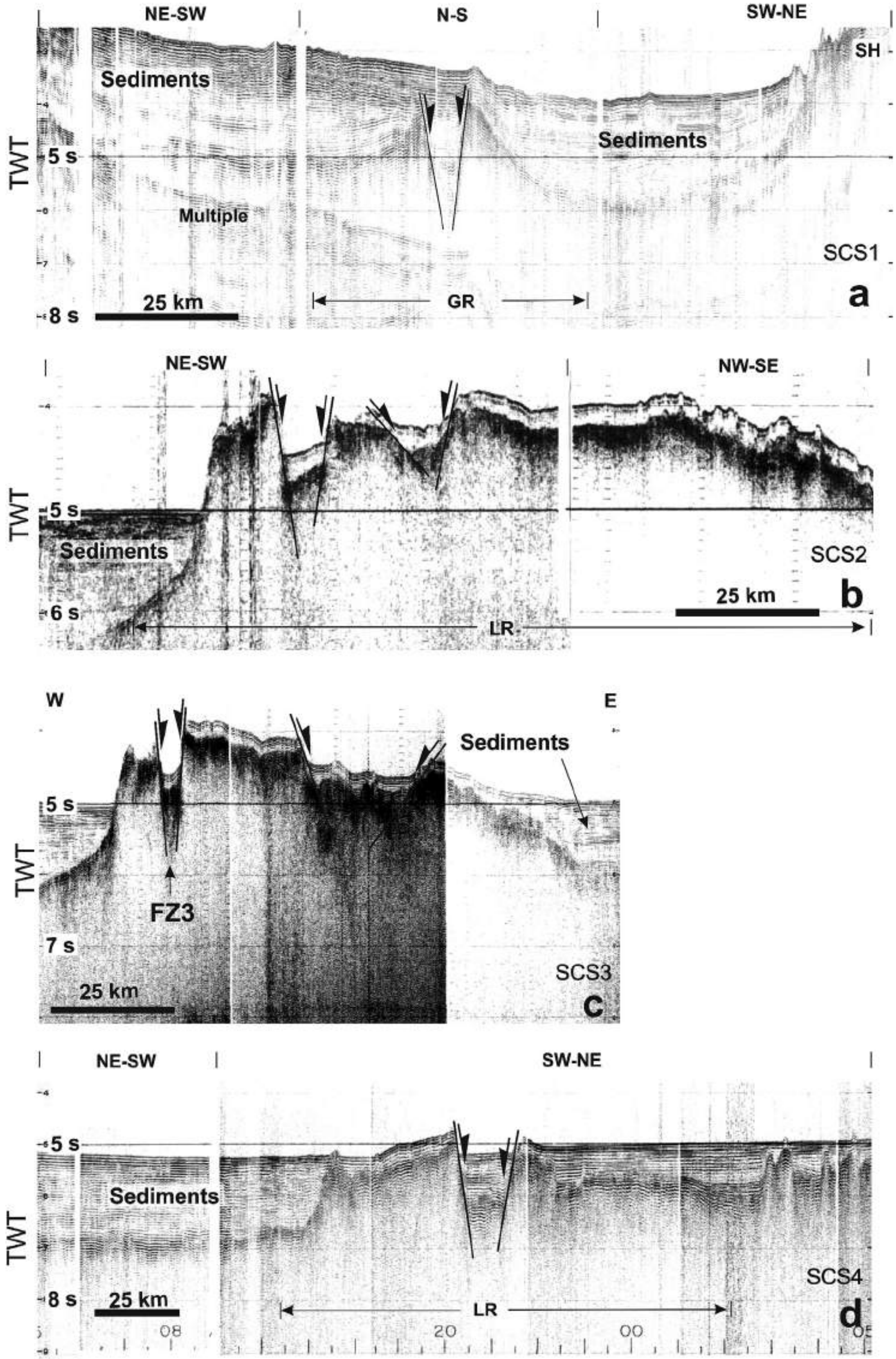

Figure 4. The vintage single channel seismic (SCS) sections show *(a)* the Gop Rift N to the Saurashtra High (Fig. 2 shows location); *(b)–(c)* the fault bound rift valleys G2 and (d) G3 atop the Laxmi Ridge. The rift valleys are clearly under-filled and contain only deep water marine sediments. Fig. 12 shows the location and the trend of the faults. GR = Gop Rift, LR = Laxmi Ridge; FZ3 = Fracture Zone between G2 and G3; TWT = Two Way Time. See sub-section 4.2 for details.

'Saurashtra Volcanic Platform' (Calvès et al., 2008; Corfield et al., 2010; Calvès et al., 2011, Fig. 2). The platform is characterised by negative free air gravity anomalies. There is also a narrow promontory, the 'Saurashtra High' (Calvès et al., 2011, Fig. 2), evident from bathymetry and free-air gravity anomaly data.

2.3. Magnetic studies

Bhattacharya et al. (1994) modelled sea floor spreading anomalies in the southern part of the Laxmi Basin by ~ NW-SE magnetic anomaly stripes. Talwani and Reif (1998) re-appraised this

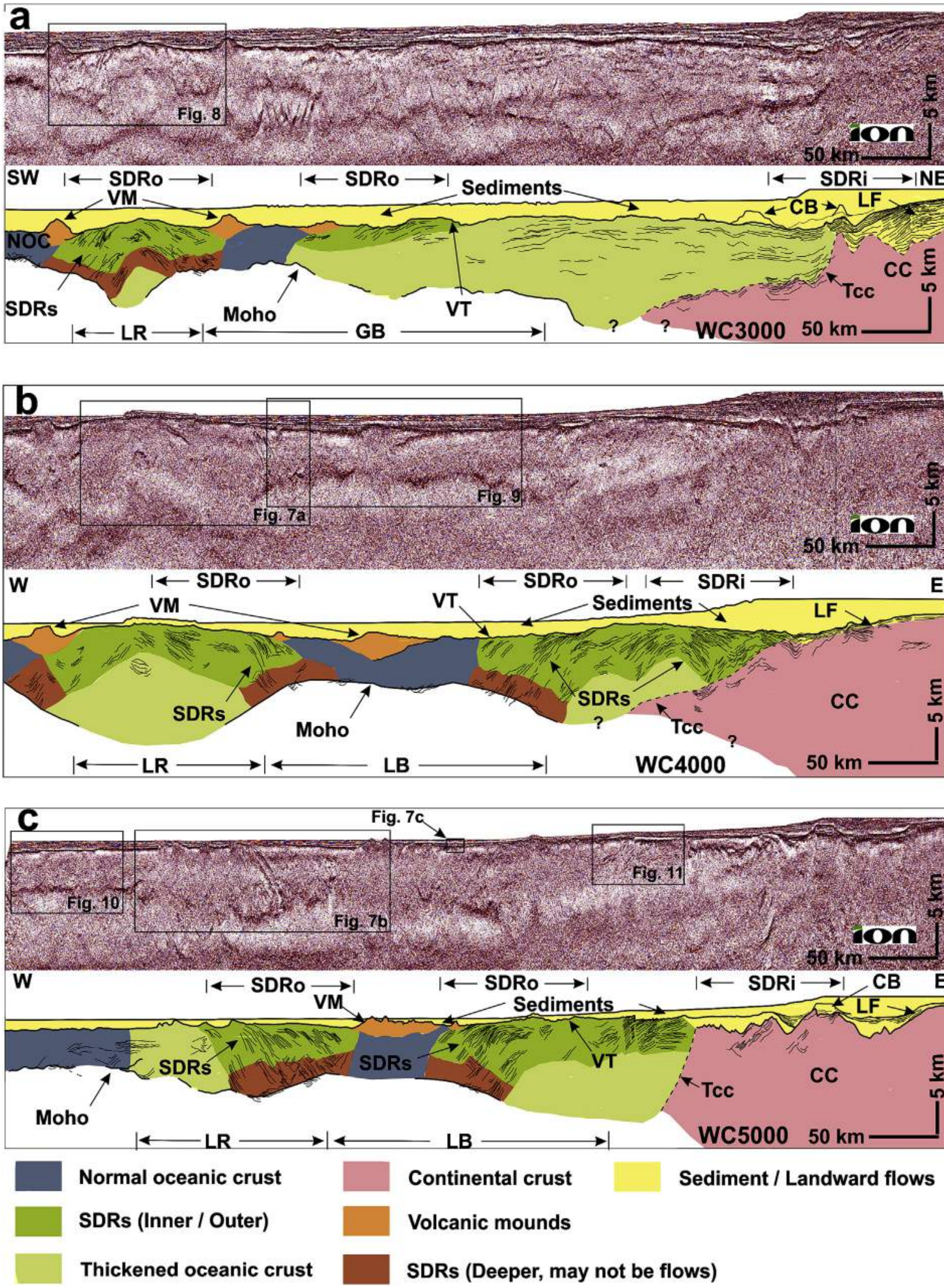

Figure 5. Ion-GXT seismic sections (top) with line drawing and crustal interpretation (below). CB = carbonate bank, VM = volcanic mound, VT = volcanics top, GB = Gop Basin, LR = Laxmi Ridge, SDRs = Seaward dipping reflectors, CC = continental crust, Tcc = Possible top of continental crust (metamorphic basement in this case); *(a)* line WC3000, *(b)* line WC4000, *(c)* line WC5000. Fig. 2 shows locations. Black rectangles: positions of the detailed seismic sections in other figures (Figs. 7a–c, 8–11). Data presented with permission from ion-GX Technology.

magnetic anomaly interpretation. The magnetic anomalies are sub-circular and isolated (Calvès et al., 2011). Krishna et al. (2006) interpreted those as magnetic highs and lows due to intrusions and basement reliefs. Magnetic anomalies interpreted in the Western Basin are unanimous (Chaubey et al., 1998; Dyment, 1998; Miles et al., 1998; Todal and Edholm, 1998; Collier et al., 2008; Eagles and Hoang, 2014; Bhattacharya and Yatheesh, submitted) and range from chron C27N and younger (Fig. 3). Todal and Edholm (1998) interpreted magnetic anomalies in the Eastern- and Western Basins as well as over the Laxmi Ridge. Their magnetic reconstruction connoted Laxmi Ridge to bear oceanic affinity. Contrary to the accepted view of Laxmi Basn being underlain by oceanic crust, Chamoli (2009) concluded from wavelet analysis of ocean floor bathymetry that the basin is underlain by continental crust. In the Saurashtra platform region, Yatheesh et al. (2009) demonstrated two sets of magnetic anomalies with different ages, chron C28 – C26 and C31 – C26, from the same magnetic data. They suggested that the existing data is insufficient to decode unique magnetic anomalies, and that advanced techniques e.g. deep tow magnetic acquisition ought to be used.

3. Data & methods

Seismic facies analyses can identify varied volcano-stratigraphic elements (e.g. Planke and Alvestad, 1999; Calvès et al., 2011). We performed 2D forward gravity modelling on three regional dip lines (locations on Fig. 2) and corroborated those with the satellite derived free-air gravity anomaly data (= the observed gravity data).

3.1. Seismic reflection data

The single channel seismic (SCS) sections (Fig. 4) are high resolution, very shallow penetrating seismic sections but were used to interpret the basement and shallow features at a few locations (Fig. 2) alongside the multichannel ion-GXT seismic sections (Fig. 5). The SCS profiles with ~ 1–2 s two-way-time image the top of the basement. On the other hand, most of the ion-GXT seismic sections are deep enough (~25 km) to image the entire crust down to the Moho. The acquisition parameters of deep tow, 10 km-long offset, 18 s recorded two-way-time, and the energy source of the strength of 170 bar-m peak to peak were designed to ensure best possible reflectivity throughout the crust. Those are long, regional lines. The three dip lines ~ NE and ~ ENE trending WC3000, WC4000 and WC5000 (Fig. 2) of the ion-GXT data set are 632, 530 and 653 km long, respectively. We interpreted the pre-stack depth-migrated (PSDM) (Fig. 5) reflection seismic sections. The velocity data in the ion-GXT is coarse interval velocities, and seldom augment the analysis. Therefore, those data were avoided. Multichannel seismic sections, with 6 km-long offset and 7–8 s record length, acquired by Reliance Industries Ltd. to map faults e.g. of the Gop Rift (Fig. 6). Notice that faults cannot be traced on one single seismic section.

The deep seismic data shows low amplitude, high frequency seismic facies at top. The facies is ~0.5–5 km thick. This pack shows alternate low- and high amplitude reflections of substantial lateral continuity. The decrease in the overall thickness of this pack in the deep basin is evident from N to S (Fig. 5). The reflections of this pack sub-parallel and onlap over a highly undulating, high amplitude reflection beneath them. Below the bright reflection, frequency diminishes and the individual reflections discontinue laterally. However, there are high amplitude reflections of fair lateral continuity for 10s of km that dip towards or away from the Indian subcontinent. These reflections either parallel or diverge down-dip. There are other very bright reflections of limited lateral continuity of ~ 5–10 km. *A* > 10 km deep bright reflections with little lateral continuity is observed in all the seismic sections (Fig. 5). Below the Laxmi Ridge, these reflections persist at deeper levels. Corfield et al. (2010) analysed the same data set. Note that though the data is of high quality, it contains numerous geophysical artefacts such as side-swipes, multiples, migration smiles.

3.1.1. Seismic interpretation

Seismic facies analysis through interpretation of various volcanic/sedimentary landforms and the Moho was performed primarily to understand the crustal architecture (e.g. Nemčok et al., 2013) and thus to provide an input for the forward gravity modelling along

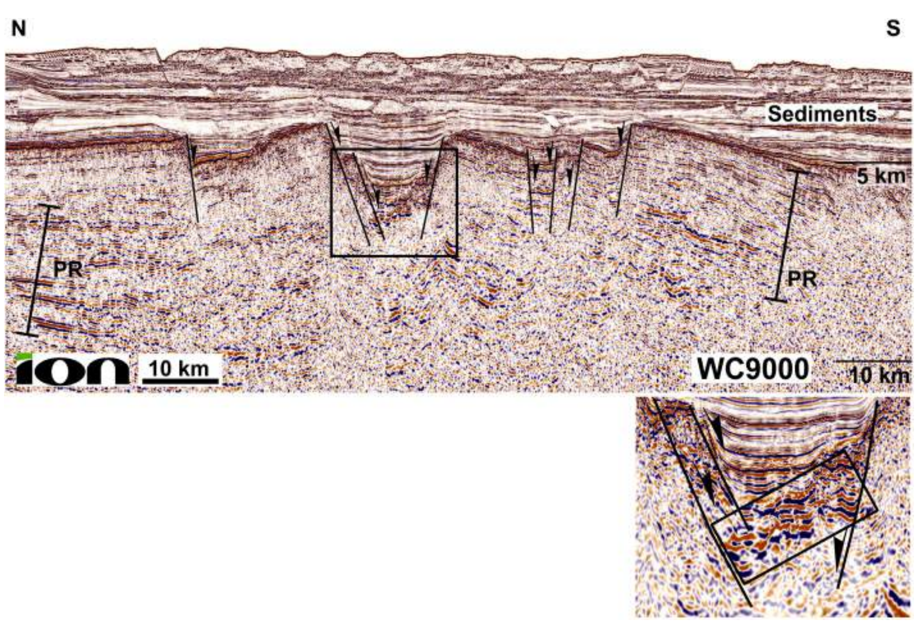

Figure 6. Part of the seismic line WC9000 (location in Fig. 2) shows the Gop Rift. No syn-rift sediments observed. The symmetric nature of the faults on either side of the central rift valleys on an oceanic crust indicates an oceanic spreading centre. See sub-section 4.1 for details. Fig. 2 shows the trend of the Gop Rift. Data presented with permission from ion-GX Technology. Inset: Details of the volcanics (as high amplitude, low frequency) in the central valley. PR: Parallel reflections.

selected profiles (locations in Fig. 2). In certain parts of the ion-GXT sections, the Moho is not visible due to greater thickness of volcanics above. For example, in Figure 9 the Moho is invisible ('blanked') beneath the volcanic mound. Sediment packs are identified on the seismic sections by their seismic facies viz. high frequency, lateral continuity of individual reflectors, overall low amplitude, cyclic high/low amplitude reflectors etc. The pack thins considerably towards S, due to the falling influence of the Indus delta (Whiting et al., 1994; Clift et al., 2002). See decreasing thickness of the seismic facies 'sediments' from Fig.5a–c. The basement i.e. the top of volcanics underlying sediments is a bright/high amplitude reflection. It lies above the seismic facies characterised by low frequency, reflections with insignificant lateral continuity etc. Local Seaward Dipping Reflectors (SDRs) manifest as continuous individual intra-basement reflectors for 10s of km. The depth of the basement is shallow (~50 m) near the coast and is much deeper (~6 km) W of Laxmi Ridge. We avoided erroneous interpretation of the seismic noisy artefacts.

3.1.2. Volcanic seismic facies analysis

We adopted standard seismic interpretation schemes for volcanic landforms (Planke and Eldholm, 1994; Symonds et al., 1998; Planke and Alvestad, 1999; Planke et al., 1999, 2000; Calvès et al., 2011; see Figs. 5-11) and use them for crustal architecture identification. The seismic volcano-stratigraphic features observed are Inner and Outer SDRs and landward flows (Figs. 5a–c), isolated volcanic mounds (Figs. 5a–c), and intrusions (Figs. 10, 11). Most of the crustal features evident on the reflection seismic sections are volcano-stratigraphic features/structures besides sediments. Also, the basement top and the Moho are evident in all the seismic sections as bright reflectors. The petrologic Moho is a geophysical boundary, and is imaged on reflection seismic sections as a single or a band of high amplitude reflectors, usually discontinuous (Rosendahl et al., 1992). The Moho beneath the oceanic crust is usually imaged as ~12–14 km deep horizontal reflections (Singh, 2011). Beneath the continental crust, the Moho reflection appears as a landward (i.e. towards ~ NE to E) dipping reflections deepening from ~12 to 14 to ~30–40 km (Rosendahl et al., 1992).

(i) Inner and Outer SDRs

Seaward Dipping Reflectors (SDRs) is a geometric term for seaward inclined, planar to arcuate reflections commonly seen in almost all magma-rich passive margins (Planke and Eldholm, 1994; Planke et al., 2000). SDR complexes (Fig. 5) are classified as Outer (submarine) and Inner (sub-aerial/neritic) depending on where they emplaced (Planke et al., 2000). The Inner and Outer SDRs resemble in seismic reflection characters (Planke et al., 2000). Both of them are topped by high-amplitude generally smooth reflections, onlapping or concordant with the overlying reflections and have usually a poorly defined base (Planke et al., 2000 and references therein). The Outer SDRs are arcuate- (convex upwards) divergent downwards while the Inner SDRs may be arcuate- (convex/concave upwards) or planar-divergent downwards. The Inner SDRs are > 6 km thick and generally dip < 15° (Planke et al., 2000). Each individual package of Outer SDRs are 2–4 km thick but they may reach > 10 km depth in a ~ 10–13 km thickened oceanic crust (Lunnon et al., 2005; this study). Inner SDRs may be mixed with sediments (Planke et al., 2000; Franke, 2013; Zou, 2013), and thus are sometimes of lower densities (2.5–2.6 g cc^{-1}) than lava flows (Planke and Eldholm, 1994). Outer SDRs have not been drilled till date so actual densities are unknown. Their densities may be more (~ 2.7–2.8 g cc^{-1}) than Inner SDRs since they are deep marine flows and may have minor interflow of pelagic/hemi-pelagic sediments.

Whereas Inner SDRs are generally underlain by continental crust, Outer SDRs are underlain by oceanic crust. Outer SDRs have been identified on oceanic crust in a number of studies (e.g. Namibian margin: Bauer et al., 2000; South Atlantic Margins: Jackson et al., 2000; SE Greenland margin: Hopper et al., 2003; N Atlantic: Lunnon et al., 2005; Argentinean margin: Franke et al., 2010; Labrador Sea in W Greenland: Keen et al., 2012). Outer SDRs have been observed on hotspot trails e.g. Elliott et al. (2009) for the Walvis Ridge in SE African margin. Outer SDRs are also recognised in oceanic crust thickened by mantle plumes. For example, the Iceland mantle plume was attributed to the thickened oceanic crust and occurrence of outer SDRs N of Faroes margin (Lunnon et al., 2005).

Seaward dipping reflectors (SDRs) persist in all of the seismic sections. The Inner SDRs are observed typically landward and overlie the possible continental crust, and are < 5 km thick (Fig. 5). Outer SDRs were identified earlier from the study area (Samal et al., 2011). We identified the Outer SDRs from the depths they reach, less individual reflection package thickness, overall less continuity than the Inner SDRs and high (> 45°) dips (Fig. 5a). The Outer SDRs reach > 10 km depth and even seem to extend ~ 2–3 km away from the Moho (Figs. 5, 7, 8). The Outer SDRs emplace atop oceanic crust. Although deepest SDRs within 2–3 km of the reflection Moho are geometrically inclined reflection packages (alike flow related SDRs), they may actually be dykes belonging to a lower oceanic crust. Therefore, flows may be absent in the deeper parts. So, we separated them as "Deeper SDRs" (Figs. 5, 7, 8).

(ii) Axial magma chambers

Axial magma chambers/melt lenses are chambers of magma feeding melt into the ridge axes of Mid-Oceanic Ridges (MORs). They have been imaged on seismic sections on many active MORs elsewhere (Detrick et al., 1987; Collier and Sinha, 1990; Mutter et al., 1995; Canales et al., 2006; Singh et al., 2006). After being abandoned due to ridge jumps, magma chambers/melt lenses solidify. However, they retain their enclosing 'conductive boundary layer' (Gillis, 2008). This layer separates them from the sheeted dyke complex on top. The dyke complexes are parts of the ophiolite successions. The magma chamber/melt lens eventually forms a closed system where high temperature hornfels facies metamorphism happens at water-under-saturated conditions (Gillis and Coogan, 2002). This recrystallizes the basaltic 'crystal mush' in the magma chamber into pyroxene hornfels and hornblende hornfels. These metamorphic processes were studied on magma chambers/melt lenses outcropping at Oman ophiolites, Cyprus ophiolites etc. (MacLeod and Yaouancq, 2000; Gillis, 2008). The resulting lithologies are denser (~ 2.9–3.4 g cc^{-1}) and provide a higher impedance contrast to image them underneath fossilized MORs on reflection seismic data. They appear as high amplitude, low frequency lensoid reflections ~ 3–5 km beneath the axes of fossilised MORs. Axial magma chambers are thus seen on two (WC3000 and WC4000) of the three presented seismic sections (Figs. 7a, 8).

(iii) Landward flows

Landward flows are identified on seismic profiles as sheet-like, wavy reflections wedging out landwards (Fig. 5). They typically lie on the continental crust, may underlie Inner SDRs and may terminate against basement escarpments (Planke et al., 2000). They are volcanics-sediments mixtures and have typical sediment like densities. They are differentiated from SDRs on seismic sections by their landwards locations, shallow depths (~5–6 km) and

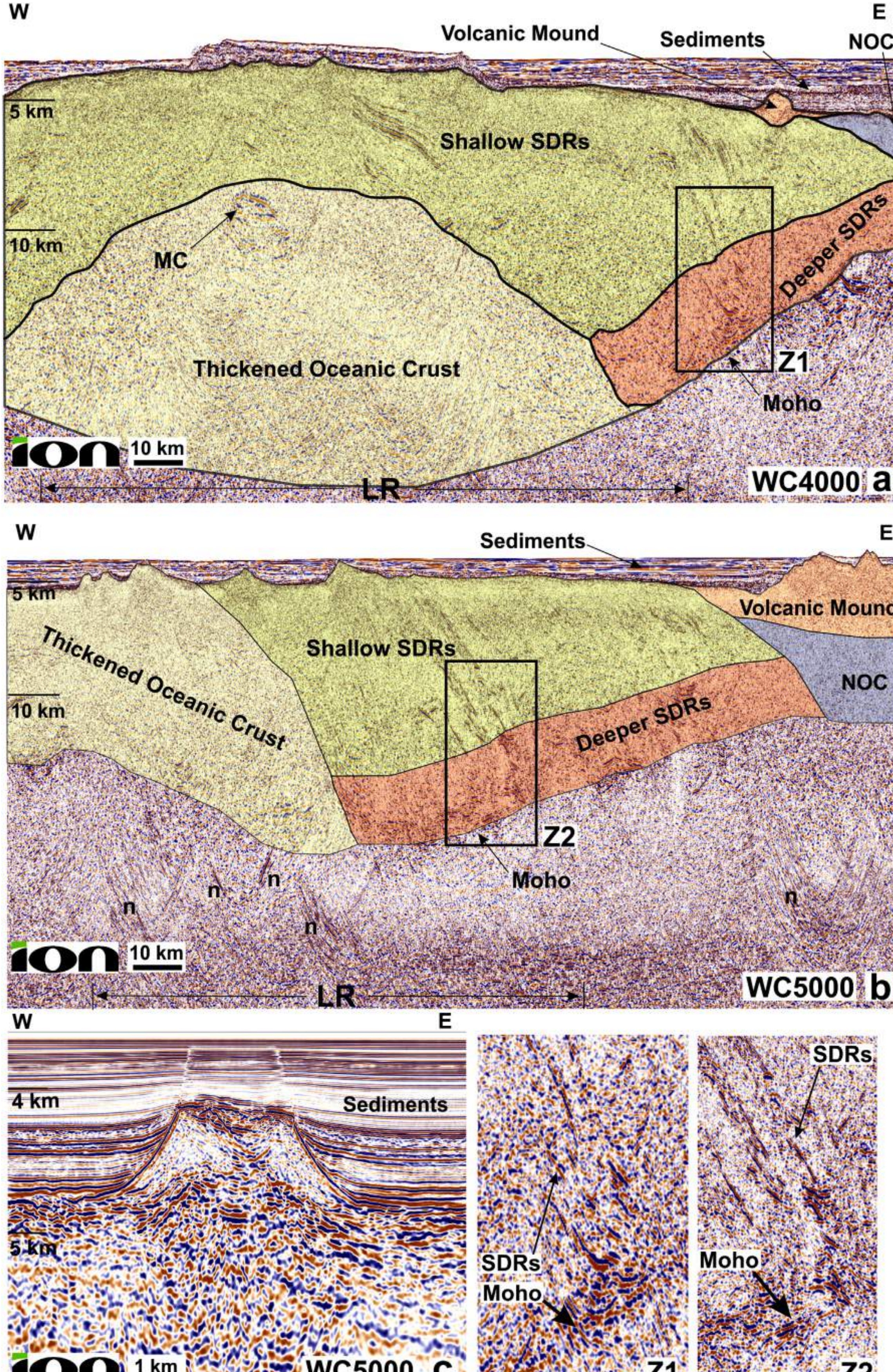
W
E
Volcanic Mound
Sediments
NOC
5 km
Shallow SDRs
10 km
MC
Deeper SDRs
Thickened Oceanic Crust
Z1
Moho
10 km
WC4000 a
LR
W
E
Sediments
5 km
Volcanic Mound
Thickened Oceanic Crust
Shallow SDRs
NOC
10 km
Deeper SDRs
Z2
Moho
n
n
n
n
n
10 km
WC5000 b
LR
W
E
4 km
Sediments
5 km
1 km
WC5000 c
SDRs
Moho
Z1
SDRs
Moho
Z2

remarkable continuity of individual reflections for up to 100 km (Fig. 5a–c).

(iv) Other volcano-stratigraphic facies/structures

Volcanic mounds often form by flexing pre-existing oceanic crust (Fig. 9). Deformation sometimes aligns minerals in a preferred orientation forming tectonic foliations. However, this was not possible to decipher from the present seismic data/interpretation. The Moho is sub-horizontal and sub-parallels the basement top, with sub-horizontal reflections, possibly because of basaltic flows, of ~ 5–8 km thick 'normal' oceanic crust nature in the Western Basin (Fig. 10). Dipping high amplitude reflections ('INT' in Fig. 10) are concave gently towards W, of ~ 2.5 km length; and could be shear-zones (e.g. Kodaira et al., 2014). The volcanic mounds (Figs. 7–9) differ from the carbonate banks ('CB' in Fig. 5) in their distinct seismic character. Carbonate mounds have basement parallel reflectors of alternating high and low amplitudes (e.g. Biswas and Singh, 1988 from the same area). In contrast, volcanic mounds have either uncharacteristic interior reflection if submarine, or appear prograding deltaic if neritic (Planke et al., 2000; Calvès et al., 2011). The volcanic mounds we found in the area are mostly of the former type (Fig. 9).

Sub-horizontal- and low dipping volcanic flow reflections, again sub-parallel to the basement top are good indicators of the oceanic crust (Planke et al., 2000; Calvès et al., 2011). We also identified a > 8 km 'thick' oceanic crust showing sub-parallel reflections (Figs. 5a,c) or have weak reflectivity (Figs. 5b,c). They underlie the Outer SDRs at most locations. They may indicate the pre-existing oceanic crust over which the voluminous SDR flows emplaced or thickening of the crust by underplating especially below the ridge and adjoining areas.

Intrusives (Figs. 10, 11) are also fairly common in the seismic sections. They appear as high amplitude, low frequency reflections. They may indicate dykes where they are sub-vertical. These schemes were used to interpret the geological nature of the Laxmi Ridge, Laxmi Basin and the Gop Rift in the sub-sections below.

3.2. Gravity- & magnetic data

The satellite free air gravity anomaly data (Fig. 2) we interpret and analyse is the compilation version 18.1, 1 min grid from Scripps Institute of Oceanography (Sandwell and Smith, 2009). The satellites (ERS-1 and Geosat) acquiring this data have gravity field measurement accuracies of 6–10 mGals and 2-4 mGals when compared with ship-track gravity (Sandwell and Smith, 2009). There is no ship track gravity for the ion-GXT lines. The magnetic grid (Fig. 3) obtained from National Geophysical Data Centre (Maus et al., 2007) was used to interpret the magnetic anomalies. The magnetic grid (EMAG3, version 1.1, 3 min grid) has large data gaps of ~100 km (Fig. 3) in the continental shelf and does not cover the ion-GXT lines. So the magnetic data was not used to model the magnetic susceptibility response of the crustal layers. Interpolation of the total magnetic intensity values in space is not viable since the region experienced multiple episodes of volcanism related to plume from 65 to 60 Ma (e.g. Chenet et al., 2007; Collier et al., 2008; Ganerød et al., 2011) and continental breakup (e.g. Collier et al., 2008). The sub-circular and isolated anomalies in the Eastern basin are related to intrusives and undulating sea floor (Krishna et al., 2006). Since the undulations and intrusives are domal as seen on gravity anomaly data (VM in Fig. 2), the magnetic response is expected to change substantially within short horizontal distances.

3.3. Gravity interpretation & modelling

3.3.1. Gravity anomaly maps

The free air gravity data (Fig. 2) shows the major tectonic elements as characteristic gravity highs and lows. N to the Laxmi Ridge, the Saurashtra Volcanic Platform (SVP in Fig. 2) shows gravity low with ~ NE trending linear gravity highs. Note that this trend parallels those of the Saurashtra High and the Gop Rift (SH and GR respectively in Fig. 2). The continental shelf edge is marked by a pronounced gravity high and the end of the slope by a prominent gravity low. The Bombay High (BH in Fig. 2) is evident as a large sub-circular gravity low. Large isolated sub-circular gravity highs indicate volcanic mounds (VM in Fig. 2). The oceanic domain SW to the Laxmi Ridge is featureless on the free-air gravity data (Fig. 2).

Bathymetric data reveals that the G2 rift valley trends ESE (Fig. 12a). Band pass filtered (10–200 km) Bouguer gravity anomaly map reveals trends of all the three G1, G2 and G3 rift valleys/grabens along with the interpreted ~ NE trending fracture zones (Fig. 12b). These grabens also can be visualised on horizontal gradient- (Supplementary Fig. 1) and vertical derivative- (Supplementary Fig. 2) of band pass filtered (10–200 km) Bouguer gravity anomaly data. Also, they can be interpreted on high pass filtered (30 km) Bouguer gravity anomaly data (Supplementary Fig. 3). The vintage SCS section reveals these ESE trending rift valleys (Fig. 4) and possibly one such NNE trending fracture zone (Fig. 4c).

3.3.2. Gravity forward modelling

2D forwards gravity modelling (Fig. 13) was performed on the interpreted seismic sections WC3000, WC4000 and WC5000 to study the crustal nature of the Laxmi Basin and the Laxmi Ridge, and whether they match the observed gravity i.e. the satellite free-sir gravity anomaly data. Jacoby and Smilde (2009) presented the principles of modelling. These lines were good candidates for the gravity model because the Moho was imaged quite well along most parts of them. This was in addition to other features viz. resolution, frequency of the data, which control the interpretation. The Moho is not imaged in the deeper parts beneath the Laxmi Ridge on these seismic lines. We used seismic refraction points (Naini and Talwani, 1982 and references therein) for depths to the Moho at available locations. We found that the 'long-range' locations L-02, 04, 05, 06, 07, 09 and 10 are only useful because those are deep enough. The minimum estimated Moho depths at those locations are 11.9, 17.9, 22.9, 17.3, 16.3, 15.1 and 19.8 km, respectively (Naini and Talwani, 1982). All these locations are labelled in Figures 3 and 13. Table 1 presents densities for the different crustal layers and sediments used in gravity modelling. We used slightly higher density of the lithospheric mantle (3.36 g cc^{-1}; lowest row in Table 1) following the densities recently used in the Eastern continental margin of India (Nemčok et al., 2013). We also trialled a lower density (3.30 g cc^{-1}) on one line (WC4000; vide Supplementary Fig. 4). We attained a good match here by lowering

Figure 7. Detail seismic sections in Figs. 5. (a–b) shows the nature of the SDRs. The SDRs clearly reach near the Moho. LR = Laxmi Ridge, MC = Magma Chamber, n = noise. (c) A small (volcanic) mound with no flexing effect on the pre-existing oceanic crust where it emplaced. The mound can be considered a cross-cutting element, the dragged sediments as host fabric element, and together they form flanking structure (Mukherjee and Koyi, 2009; in press). Location of (c) is shows in Fig. 5c. Data presented with permission from ion-GX Technology. Z1, Z2: zoomed sections from the corresponding numbered rectangles in *(a)* and *(b)*. These sections show SDRs close to Moho. The reflections crossing the Moho may be noise in the seismic data.

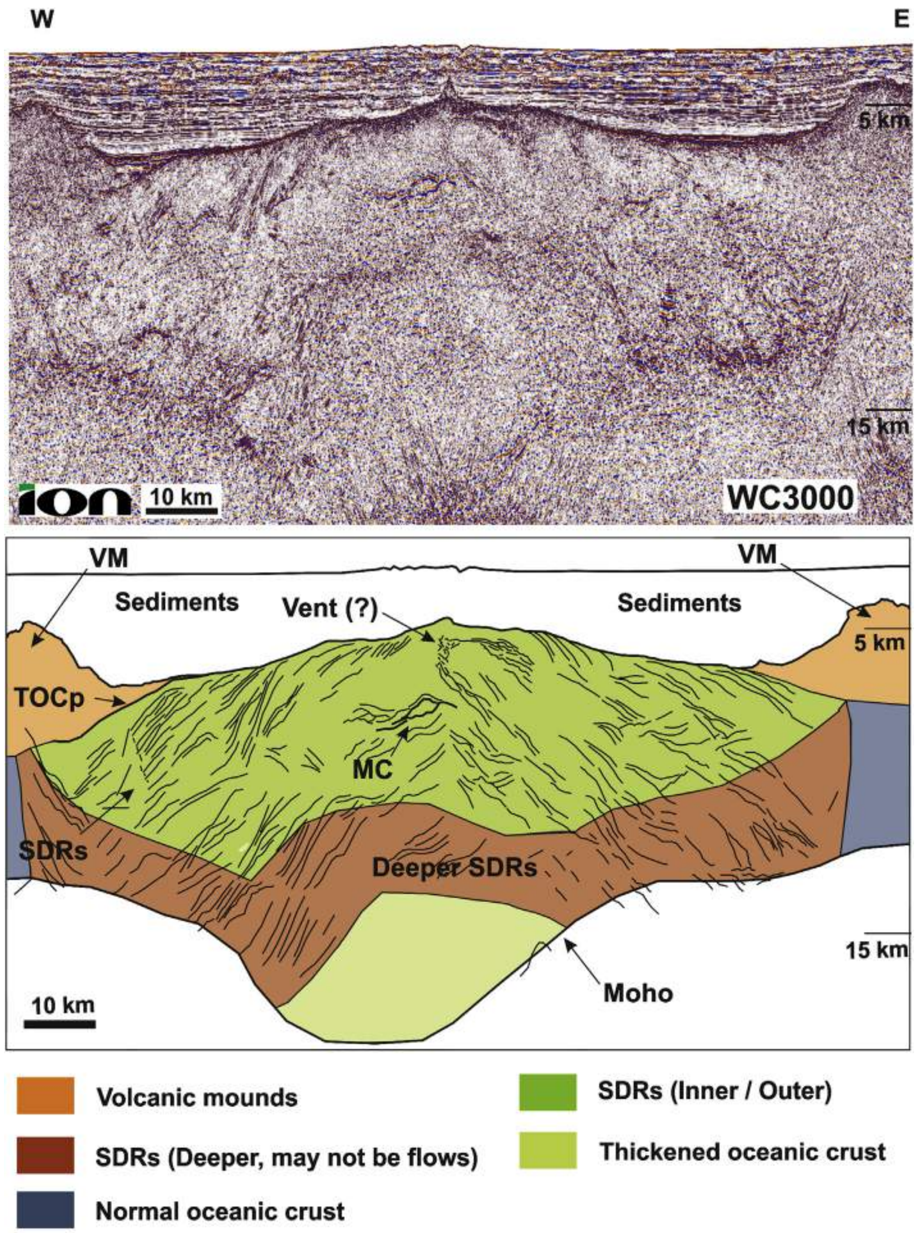

Figure 8. Detail of the Laxmi Ridge seismic volcano-stratigraphy (top) and interpreted line drawing and crustal architecture interpretation (below) shows the SDRs and the deeper SDRs, MC = Magma Chamber. Detailed at sub-section 3.1.2. Location of seismic section in Fig. 5a. Data presented with permission from ion-GX Technology. The reflections crossing the Moho may be noise in the seismic data.

the densities of only two layers on top of the Laxmi Ridge, each by a miniscule 0.05 g cc^{-1} (compare Fig. 13b with Supplementary Fig. 4). This shows that either of the two mantle densities can be comfortably used for the Laxmi Ridge gravity models. We considered sediments of three or four layers depending on the total thickness of the sediments above the basement. The SDRs were modelled as layers with lower densities (2.7–2.8 g cc^{-1}) in the 2D gravity modelling. The results are presented in Figure 13a–c. Models on the lines WC3000 and WC4000 match well between the observed and calculated gravity (root mean square error < 3.0), and the line WC5000 too shows a match (root mean square error ~ 5). Line WC5000 does not show an excellent match since it locates between two gravity lows and at the edge of one of the lows (Fig. 2). Thus, the gravity effects in 3D influence the gravity signal, which cannot be modelled in 2D.

3.4. Magnetic interpretations

We interpreted some linear magnetic trends in the Saurashtra Volcanic Platform and in the Gop Rift region (Fig. 3). There are two anomalies of same trend W of the seismically identified Gop Rift (vide sub-section: 4.1) and on either sides of it. The two anomalies are equi-spaced: ~ 50 km N and S of the Gop Rift (Fig. 3). These magnetic anomalies were interpreted to be due to basement reliefs on a ~ 100 km wide single reverse-polarity block (Minshull et al., 2008). These indeed coincide with gravity highs and lows (Fig. 3) indicating possible basement undulations. Even if they are real, assigning ages to the magnetic anomalies would be difficult (Yatheesh et al., 2009).

Note that the 110-120° N trend of the three rift valleys- G1, G2 and G3-within the Laxmi Ridge match with those of the magnetic

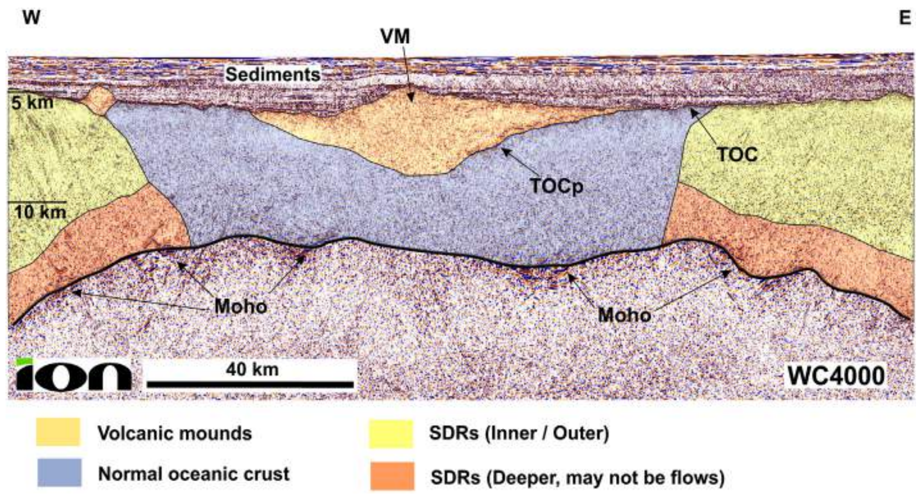

Figure 9. Detail of a volcanic mound (VM) on seismic section in Fig. 5b. The pre-existing oceanic crust top (TOCp) flexed by loading. The Moho lies sub-horizontal beneath and the oceanic crust has a 'normal' thickness. See sub-section 3.1.2 for details. VM = Volcanic Mound; TOC = Top of oceanic crust at present. Data presented with permission from ion-GX Technology.

anomaly for chron C27N (compare Figs. 3, 12b). This also implies that the Seychelles microplate moved towards ~ SSW.

4. Results

4.1. The Gop Rift & the Laxmi Basin

The Gop Rift at SE shows low gravity anomalies on free air gravity data with isolated high gravity anomalies (labelled VM in Fig. 2). The regional seismic profiles show volcanic mounds with clear flexure of the top of the pre-existing oceanic crust (Fig. 9). Such flexures of the oceanic crust due post-dated loads are commonly seen at the Canaries, Hawaii and Marquesas (Watts, 2001). Note that those > 5 km high loads are large enough to undulate the Moho. In our case, the ~ 2.5 km high load is either not that large or composes low-density hyaloclastites (Planke et al., 2000) and does not arch the Moho. The volcanic load atop the oceanic crust, thus, post-dates the oceanic crust. Thus, the oceanic crust did not originate at the mound. The Gop Rift was considered to continue as an NNW-SSE extinct spreading centre (GRp in Fig. 2) connecting the isolated mounds Wadia Guyot, Panikkar - and Raman Seamounts (Bhattacharya et al., 1994; Talwani and Reif, 1998; Krishna et al., 2006). But, our analyses on the high resolution seismic data show that these are isolated, sub-rounded seamounts most possibly formed as volcanic cones. So, the extinct ridge does not exist between the Laxmi Ridge and the W continental margin of India.

In the ion-GXT seismic line WC5000, we deciphered an oceanic fracture zone (similar to p. 364 of Watts, 2001, Fig. 11). We call this the '*Ratnagiri Fracture Zone*' ('RFZ' in Figs. 2, 11). Towards E, Ratnagiri is the nearest well known locality onland. The ~ NNW trend of the RFZ has been mapped from other shallow 2D seismic lines (Fig. 2). The RFZ is > 200 km long with ~ 70 km in width. The N and S are limited by data availability. The dip of the main 'fault'

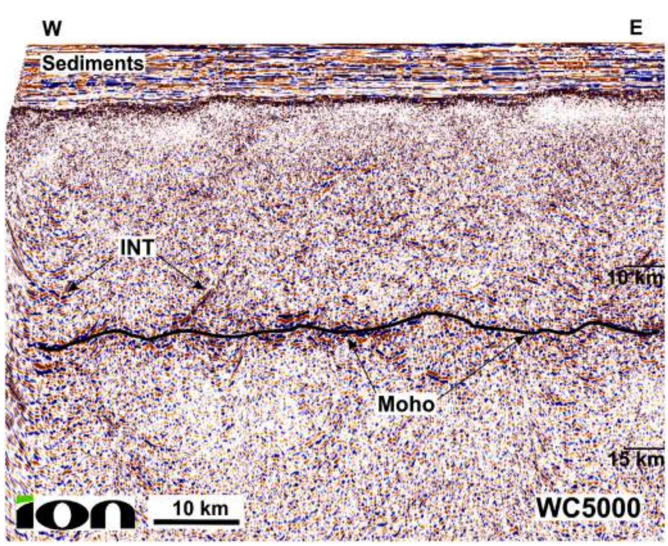

Figure 10. Seismic volcano-stratigraphy of the 'normal' oceanic crust in the Western Basin (location in Fig. 5). INT = Intrusive: possibly dykes, high amplitude, low frequency and angular relationship with surrounding reflections; possibly, intruded fault/shear planes (e.g. Kodaira et al., 2014). The Moho is flat and the seismic reflections in the top part of the oceanic crust are sub-horizontal because of flows. Below that they are sub-horizontal/wavy due to intrusions. Data presented with permission from ion-GX Technology.

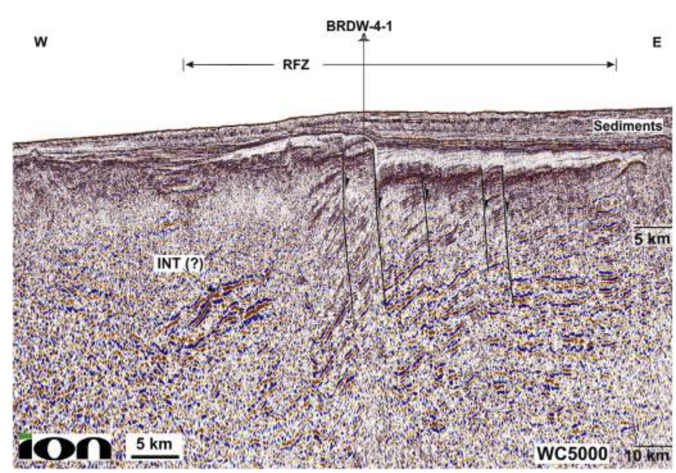

Figure 11. Detail of the Ratnagiri Fracture Zone (RFZ) observed in E–W seismic section with the well BRDW-4-1. The largest throw on these faults is ~1.5 km. Fig. 2 shows the NNW-SSE trend of the Ratnagiri Fracture Zone. Location of seismic section in Fig. 5c. Data presented with permission from ion-GX Technology. The possible intrusions (INT) indicated by high amplitude, low frequency and angular relationship with surrounding reflections: those could be dykes or intruded fault/shear planes.

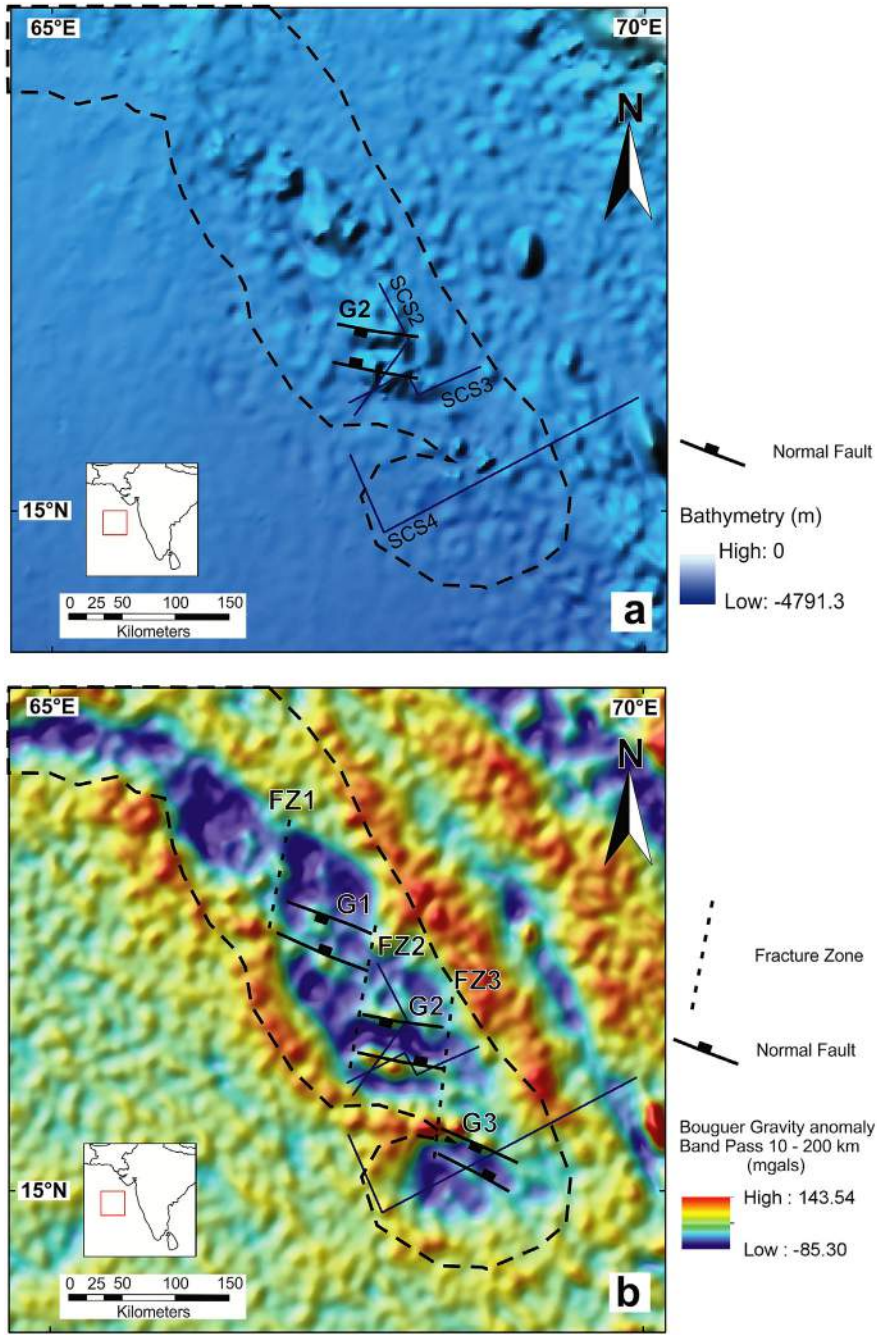

Figure 12. Map shows the trends of the fault bound rift valleys/grabens (G1, G2 and G3) on the Laxmi Ridge observed on *(a)* bathymetry, and*(b)* and pass (10–200 km) filtered Bouguer gravity anomaly data (density of Bouguer slab = 2.67 g cc^{-1}). Thin lines with 'SCS' prefixed labels: SCS profiles.

(actually, fracture zone) i.e. the one with the largest 'throw' (rather, scarp height) on this line is ~ 60°. The E block experienced more cooling-related subsidence because it is possibly older than the W block (see Watts, 2001). Note, reverse dragged units (Mukherjee and Koyi, 2009; Mukherjee, 2013, 2014, in press) near the fracture zones. But, there should not be any slip on these fracture zones (Hall and Gurnis, 2005). The 'apparent' slip is due to the differential subsidence on either sides of the fracture zone. To maintain the scarp height due to the age difference, the blocks flexed (p. 363–364 of Watts, 2001; Hall and Gurnis, 2005). This flexure appears as reverse drags against the fracture zones. There are eastward bend of the top of the seismically transparent horizon over the fracture zones. The bend is maximum on the main fracture zone i.e. the one with the largest scarp. The continuing differential subsidence on these fracture zones is indicated by these bends on the fracture zones. The segments of the RFZ are named 'a'-'d' from N to S (Fig. 2). Their inferred lengths are ~50, 120, 50 and 60 km, respectively. The spacing between 'a' to 'b', 'b' to 'c' and 'c' to 'd' segments are ~40, 10 and 20 km, respectively. They trend WNW-ESE: same as that of the Indian shelf. This trend represents approximately the spreading direction. This means that this segment of the margin is *'hyper-oblique'* (e.g. Baudot et al., 2013). We did not observe any spreading centre between the segments of the RFZ on the present data. Had there been any spreading centre, it would had been perpendicular to the RFZ i.e. ENE-WSW. This trend of the possible spreading centre related to the RFZ, matches well with our mapped Gop Rift (Figs. 2, 3). The tectonic elements: the Gop Rift and the RFZ formed possibly during the same sea floor spreading episode. The RFZ sub-parallels the extinct spreading centre in prior studies (GRp in Fig. 2). It is impossible for a spreading centre to parallel the related fracture zone. Thus, it further confirms that no extinct spreading centre exists, E of Laxmi Ridge. The well BRDW-4-1 drilled to 3250 m 'total depth' below sea level (NELP VII, 2007), on the up-thrown fault block W of the fracture zone encountered Early Paleocene basalts of unconstrained thickness underneath a Late Paleocene to Recent clay section.

At the northern part of the study area and at the northernmost end of the ion-GXT seismic line WC9000, normal faults dipping towards each other are evident (Fig. 6). This is the ~ NE-SW trending Gop Rift. The Gop Rift is present at the SE end on the Saurashtra Volcanic Platform and is underlain by ~18 km thick oceanic crust (Fig. 3 of Corfield et al., 2010). This is clearly a rift. Rifts are either continental or oceanic (i.e. mid-oceanic rift ridge systems). Continental rift systems invariably possess some rift related/ syn-rift sediments. Note faults continue from the volcanic basement into the sediments up to the water bottom. They are imaged as reflections but are invisible at the middle of the sediment pack. These faults may continue upwards outside the seismic resolution and thus are invisible in the current data. They might have channels above them (e.g. Coumes and Kolla, 1984; Carmichael et al., 2009) and appear to have a larger throw at the sea-bottom (Fig. 6).

On seismic sections, 'syn-rift' sediments are identified by thickening of the sediment packages towards normal faults/growth faults, roll-overs, top of syn-rift unconformities (e.g. Ravnås and Steel, 1998; Morley et al., 1999), occurring with continental rift faults detaching at 8–15 km depth. The Gop Rift shows normal faults devoid of any 'syn-rift' sediment. The Gop Rift trend matches somewhat with the Gulf of Kutch. The Gulf of Kutch and Gulf of Cambay have >3–4 km thick syn-rift sediments (Biswas and Thomas, 1992). Had the Gop Rift been a continuation of the Gulf of Kutch, it would have initiated as a sub-aerial rift and subsided to modern depths of ~ 4–5 km. In that case, it would definitely have at least 1–2 km of syn-rift sediments to match its counterparts. Rather, the seismic facies suggest a deep-water post-rift nature of the sediments filling the rift valleys and also continuing outside. It is thus highly unlikely to be a continental rift. The only other possibility is that it could be a marine rift i.e. a spreading centre. In that case, it is a slow spreading centre, because it is characterised by a 1–2 km deep and ~ 20 km wide central graben, with normal faults dipping towards each other (e.g. Morgan and Ghen, 1993; Standish and Sims, 2010; see fig. 5.9 of Frisch et al., 2011; pp. 111 of Searle, 2013). Axial ridge is not observed in this section possibly because of the spreading rate and magma supply relationship (e.g. Morgan and Ghen, 1993). We rather observe axial magmatic products (Fig. 6, inset) as high amplitude, low frequency reflections. The intra-basement reflections parallel mutually and also sub-parallel the basement top (marked as "PR" in Fig. 6). They are southward inclined volcanic flows. The inclination towards S may be because of ridge segmentation, ridge capturing due to a ridge jump or increased subsidence induced loading by sediment or volcanics. What caused this inclination remains indeterminate.

However, the Gop Rift does not continue towards SE parallelling the Laxmi Ridge (as in fig. 19 of Calvès et al., 2011). We interpreted the ~ NE trend of this rift from other shallow 2D seismic sections (GR in Fig. 2). The ~ NE trending spreading centre implies movement of the Seychelles microplate towards SE. The Gop Rift was also interpreted N of the Saurashtra High on vintage SCS sections (Fig. 4a). Thus, the Gop Rift extends for > 150 km N to the Saurashtra High.

4.2. Laxmi Ridge

Continental slivers/microcontinents are characterised by positive free-air gravity anomalies, prograding sedimentary sequences on the flanks, continental crustal structures viz. rift/growth faults and related sedimentation etc. (e.g. Rey et al., 2003; Péron-Pinvidic et al., 2010 for Jan Mayen microcontinent; Plummer and Belle, 1995; Plummer et al., 1998 for Seychelles; Borissova et al., 2003 for Elan Bank microcontinent). The Laxmi Ridge has ~ 4–10 km thick SDRs on its flanks, rift faults with < 500 m thick sedimentation (Figs. 4b–d). The Moho is seen as a flexure beneath the Laxmi Ridge. The depth of Moho deduced from seismic sections match with those obtained from seismic refraction points (Naini and Talwani, 1982) and from the seismic refraction line (Minshull et al., 2008). On the vintage SCS sections, rift valleys- G1, G2 and G3-are seen that are bound by normal faults dipping towards each other i.e. ~ SW and NE (Figs. 4b–d). These seismic facies on SCS sections show the rift valleys to be devoid of rift-related sediments (e.g. Ravnås and Steel, 1998; Morley et al., 1999). Rather they contain only deep-water sediments. This is understood by the seismic facies of the sediments i.e. cyclic bright and dim, parallel reflectors of good lateral continuity, and were correlated with well BRDW-4-1 to be clay. Such reflectors have been drilled elsewhere and pelagic to hemi-pelagic clays and calcareous-siliceous oozes were obtained e.g. by Mignot and Mauffret (1986) for SW Pacific, Rothwell et al. (1998) for N Atlantic and Murdmaa et al. (2012) for a large region in the Atlantic. The sedimentation resembles that in the Gop Rift (see sub-section 4.1 and Figs. 4a, 6) in terms of seismic facies. It shows absence of thick sediments towards normal faults and 'top of syn-rift'-/breakup unconformity. Rather the sediments in the rift valleys are same in seismic facies as those outside those valleys. This indicates the deep water post-rift nature of the entire sedimentation.

The top of the Laxmi Ridge is presently ~ 3.5–5.0 km deep with ~0.5 km thick sediments within the three rift valleys. Unfortunately, the fracture zones on the Laxmi Ridge were not imaged in the ion-GXT seismic lines. There are lensoid bodies of ~ 7 km width and ~ 1 km thickness, and are deciphered as high amplitude, low frequency reflections ~ 3 km beneath the crest of the Laxmi Ridge, observed on lines WC3000 and WC4000 (MC in Figs. 7a, 8). Such lensoid bodies are magma chambers frozen since the spreading centre was abandoned by ridge jump. See sub-section 3.1.2 for how axial magma chambers develop an impedance contrast after solidifying. Being visible on lines WC3000 and WC4000 indicates its > 200 km lateral continuity sub-parallel to the Laxmi Ridge. Magma chambers of large along axis continuity, matching 4–6 km width and 1–3 km depth, have also been identified from a number of spreading ridges elsewhere (Detrick et al., 1987; Collier and Sinha, 1990; Mutter et al., 1995; Singh et al., 2006). 10–15 km deep SDR complexes were also observed. Those either touch the Moho or reach < 2 km from the imaged Moho on the ion-GXT seismic lines beneath the Laxmi Ridge (Figs. 7, 8). As mentioned in sub-section 3.1.2, such Deeper SDRs may not be flows but could be intrusions, possibly dykes, belonging to the normal oceanic crust later thickened by voluminous lava flows depicted as the Outer SDRs.

The SDRs cannot be crustal penetrating faults because such faults happen to be listric i.e. concave upwards. These SDRs are typically convex upwards and may resemble anti-listric faults, i.e. curved fault planes with dip increasing with depth. Here anti-listric faults are unlikely since: *(a)* such listric faults occur in transpressional settings (see Morley et al., 2007). This is not our case. *(b)* Anti-listric faults sometimes branch out and diverge upwards forming "flower-structures" (Misra et al., 2009 for outcrop image, and Harding, 1985; Del Ben et al., 2008 for seismic images). The reflections here are just the opposite: they diverge downwards and

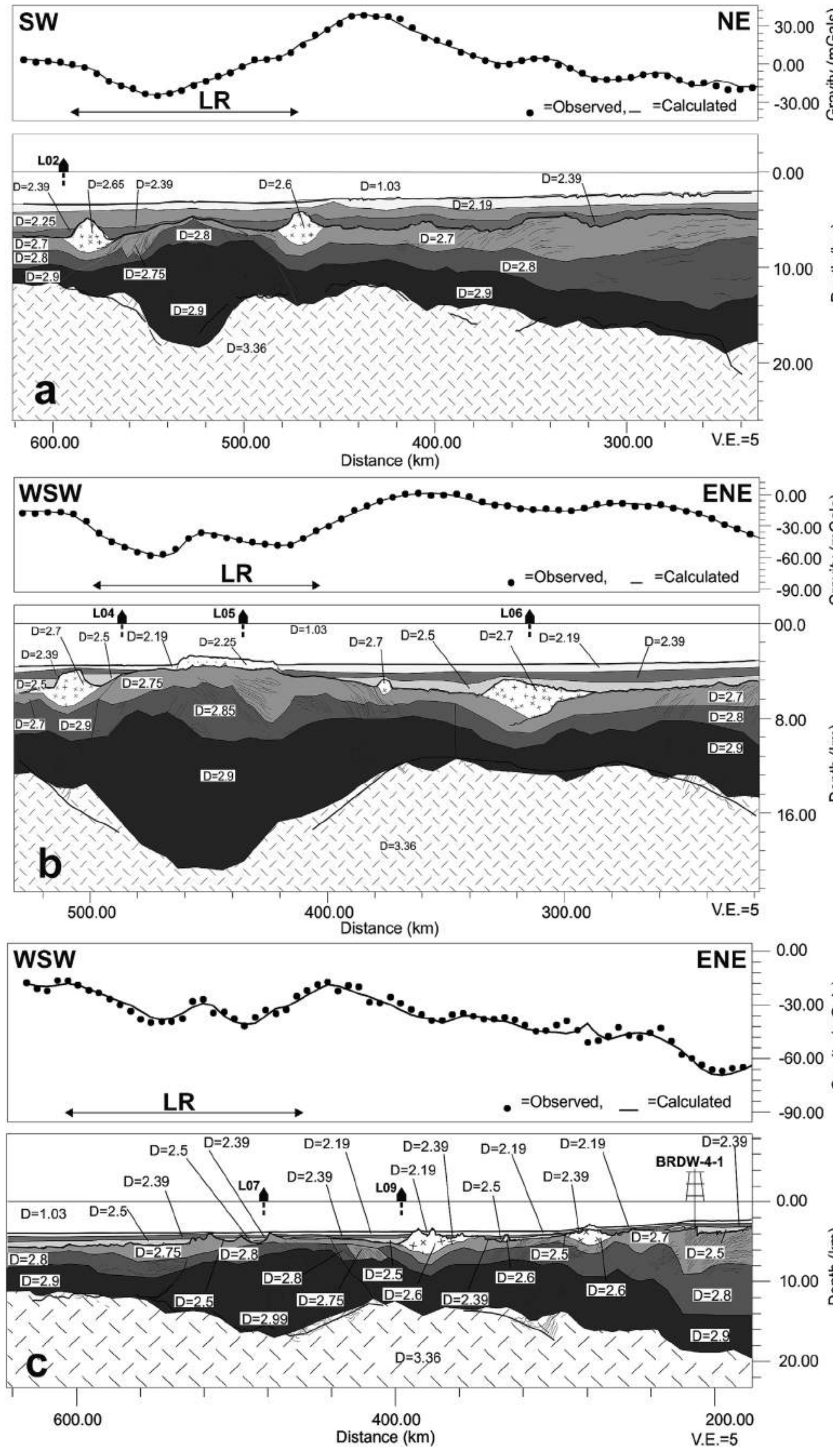
SW
NE
Gravity (mGals)
30.00
0.00
-30.00
LR
=Observed, _ =Calculated
L02
D=2.39
D=2.65
D=2.39
D=2.6
D=1.03
D=2.39
D=2.19
D=2.25
D=2.8
D=2.7
D=2.7
D=2.8
D=2.75
D=2.8
D=2.9
D=2.9
D=2.9
D=3.36
0.00
10.00
20.00
Depth (km)
a
600.00
500.00
400.00
300.00
V.E.=5
Distance (km)
WSW
ENE
0.00
-30.00
-60.00
-90.00
Gravity (mGals)
LR
=Observed, _ =Calculated
L04
L05
L06
D=1.03
D=2.7
D=2.5
D=2.19
D=2.25
D=2.7
D=2.5
D=2.7
D=2.19
D=2.39
D=2.39
D=2.5
D=2.75
D=2.85
D=2.7
D=2.9
D=2.8
D=2.9
D=2.9
D=3.36
00.0
8.00
16.00
Depth (km)
b
500.00
400.00
300.00
V.E.=5
Distance (km)
WSW
ENE
0.00
-30.00
-60.00
-90.00
Gravity (mGals)
LR
=Observed, _ =Calculated
D=2.5
D=2.39
D=2.19
D=2.39
D=2.19
D=2.19
D=2.39
D=2.39
L07
D=2.39
L09
D=2.19
D=2.5
D=2.39
BRDW-4-1
D=1.03
D=2.5
D=2.75
D=2.8
D=2.8
D=2.5
D=2.7
D=2.5
D=2.9
D=2.8
D=2.5
D=2.6
D=2.6
D=2.5
D=2.75
D=2.6
D=2.39
D=2.8
D=2.99
D=2.9
D=3.36
0.00
10.00
20.00
Depth (km)
c
600.00
400.00
200.00
Distance (km)
V.E.=5

Table 1
Densities used in the 2D forward gravity modelling (in sub-section 3.3.2). Densities used for the gravity modelling were taken from standard rock properties tables (e.g. Clark, 1966; Touloukian et al., 1981; Christensen and Mooney, 1995; Lillie, 1999). This table is used in sub-section 3.3.2 and Figures 13, 14.

Unit	Density (g cc^{-1})
Water	1.03
Sediments-1	2.19
Sediments-2	2.25
Sediments-3	2.39
Sediments-4	2.50
Upper continental crust	2.63
Middle continental crust	2.89
Lower continental crust	3.04
Upper oceanic crust	2.70–2.75
Middle oceanic crust	2.80–2.90
Lower oceanic crust	2.90–2.99
Proto-oceanic crust (and anomalous mantle)	2.99–3.2
Volcanic mounds	2.60–2.70
Lithospheric mantle	3.36

do not constitute a flower. *(c)* Anti-listric faults do not occur deeper than ~ 6 km. The ductility of the crust increases with depth and faults eventually merge tangentially at a middle crustal level of ~ 8–15 km as ductile shear planes (see Morley et al., 2007). In the present case, we observe the reflections to be steep (> 45°) and continue beyond 10 km of depth.

The gravity models show that a high density (2.8–2.99 g cc^{-1} for most part, with 2.7–2.8 g cc^{-1} for the SDRs) crust forms the Laxmi Ridge and also the Laxmi Basin. We also modelled the Laxmi Ridge with lower densities like those of a granitic crust for a sensitivity analysis of the modelling. We used 2.63 g cc^{-1} for a thinned upper- and middle crust and 2.9 g cc^{-1} for an underplated/intruded lower crust. It gave a large mismatch between the observed and calculated gravities, e.g. the root mean square (RMS) error rose to ~ 14 mGals compared to ~ 2 mGals for WC4000 (Fig. 14). Similar results also are seen for the other modelled lines (RMS errors > 10 mGals). Thus, the Laxmi Ridge is unlikely to be a thinned continental crust. The negative gravity anomaly is because of the ~ 20 km deep crust beneath the Laxmi Ridge, where 2.9 g cc^{-1} lower oceanic crustal rocks juxtapose against 3.36 g cc^{-1} mantle rocks, giving the required density contrast.

Most unanimous plate reconstructions place the Carlsberg ridge of C27 near the Laxmi Ridge (e.g. Reeves and de Wit, 2000; Royer et al., 2002). We placed the C27 (60.9 Ma) ridge of Royer et al. (2002) on the Free-air gravity anomaly data with respect to the Indian sub-continent. We also placed our interpreted Laxmi Ridge spreading centre alongside (Fig. 15). We find a good geometric match for both the ridges. The C27 ridge of Royer et al. (2002) is based on interpretations of the magnetic anomaly stripes and their deflections. Our ridge geometry is based on seismic interpretations of faulted rift valleys and possible fracture zones. A good match between these two interpretations strengthens the fact that these rift valleys (G1, G2, G3) are indeed oceanic ridge systems. Note that ridge segments undergo morphologic changes depending on spreading rate variation, mantle anisotropies, plume interactions etc. (e.g. Gente et al., 1995; Allerton et al., 2000; Bruguier et al., 2003; Mittelstaedt et al., 2008, 2011).

5. Discussions

Previous studies on the crustal nature of the Laxmi Ridge were constrained by data coverage and quality. Most of the seismic refraction points and the lone refraction seismic line lacked enough penetration of rays to image the Moho. The shallow seismic data imaged only ~ 1–2 km of the top crust and imaging Moho was impossible. Gravity inversion modelling was thus challenged in terms of constraints of the Moho depth beneath and around the Laxmi Ridge (Naini and Talwani, 1982; Bhattacharya et al., 1994; Talwani and Reif, 1998; Todal and Edholm, 1998; Krishna et al., 2006; Minshull et al., 2008). There are P-wave velocities of ~ 6.2 km s^{-1} for the middle crustal layers of the Laxmi Ridge, which indicated it to be continental crust. However, global average P-wave velocity for the middle crustal layers in rifted margins is 6.4 ± 0.3 km s^{-1} (Rudnick and Fountain, 1995 and references therein). Moreover, following the Nafe-Drake curve for compressional waves (Nafe and Drake, 1957), a P-wave velocity of 6.2 km s^{-1} relates a range of densities ~ 2.7–3.1 km s^{-1} (Ludwig et al., 1970). Again, on the linear relationship between P-wave velocity and rock density, known as the Birch's law (Birch, 1961), the density range for P-wave velocities of 6.2 km s^{-1} yielded same magnitude what we got from the Nafe-Drake curve (Nafe and Drake, 1957). Seismic signature of basalts appears complicated since they show a range of compressional wave velocities: 5.5–6.5 km s^{-1} (Christensen and Mooney, 1995). A magnitude of 6.2 km s^{-1}, thus match the range for basalts and most possibly represent lower velocities because of SDR complexes, hyaloclastites, etc. Therefore, we believe velocities cannot proxy crustal type (Christensen and Mooney, 1995). The magnetic anomalies are non-linear in the Gop- and the Laxmi Basins (Figs. 1, 3). Magnetic anomalies mask presumably due to plume and breakup related volcanics from multiple sources of varying ages. Moreover, having a sparse grid of magnetic data (Fig. 3) accentuates the problem. This is because small linear trends cannot be picked, and leads to misinterpretation. Thus, gravity- and magnetic studies, and seismic refraction velocities remained inconclusive in the previous studies (Naini and Talwani, 1982; Bhattacharya et al., 1994; Talwani and Reif, 1998; Todal and Edholm, 1998; Krishna et al., 2006; Collier et al., 2008) to decipher the crustal nature of the Laxmi Ridge, since those analyses point towards both continental and oceanic nature. 50-60 mWatt m^{-2} of heat flow on the Laxmi Ridge favour a 60–65 My old oceanic crust that has an average heat flow of 60 mWatt m^{-2}. The crustal nature of the Laxmi Ridge, thus, remained a paradox.

The high resolution seismic data from ion-GXT crucially covers the entire Laxmi Ridge and the Laxmi Basin. As mentioned earlier, crustal layers, volcanic landforms, Moho, etc. were interpreted to understand the crustal architecture and provided input for forward gravity modelling. The SCS profiles strengthened this understanding. The gravity models match between the observed and calculated gravities (Fig. 13). One line, WC5000 (Fig. 13c), does not show a good match like the other two (Fig. 13 a,b) because of the line position between two gravity lows and close to the flank of one. A well constrained 3D gravity forward model can solve such issues. Unfortunately, to the knowledge of the authors, 3D seismic data in this area is unavailable. We further comprehend that gravity modelling is non-unique. So, inferring from gravity alone Laxmi Ridge can be either oceanic or continental crust. To reduce this uncertainty, we used depths to Moho and other interfaces from industry grade PSDM seismic data and combined with seismic refraction points from previous studies to gauge the depth to the Moho along the lines. The seismic refraction points provide depths to the Moho underneath the ridge where the seismic reflection imaging is weak. Earlier authors (e.g. Bhattacharya et al., 1994; Talwani and Reif, 1998; Todal and Edholm, 1998; Krishna et al.,

Figure 13. 2D forward gravity models on parts of the ion-GXT seismic profiles. *(a)* line WC3000 *(b)* line WC4000 (c) WC5000. See sub-section 3.3 for details and Table 1 for densities of crustal layers. Refraction points (from Naini and Talwani, 1982) are numbered L02, L04, L05 etc. For depths to the Moho derived from these refraction points see sub-section 3.3.2. Thin lines: line drawing from Fig 5 overlaid.

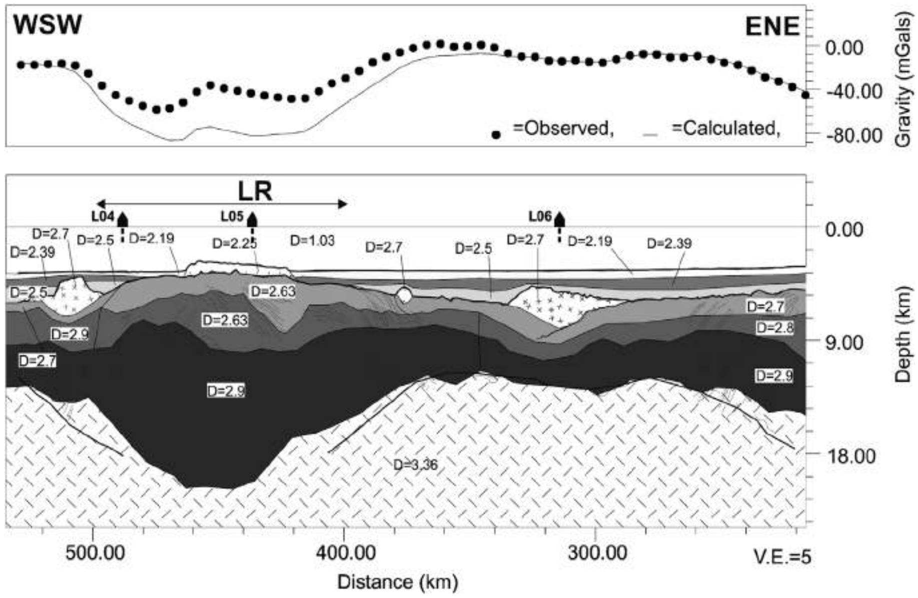

Figure 14. Sensitivity analysis of the 2D forward gravity model considering the Laxmi Ridge as a thinned continental crust. Note a large mismatch between observed and calculated gravity values on the Laxmi Ridge (RMS error: ~ 15 mgals; maximum error: ~ 40 mgals). L04, L05 and L06 are refraction points (from Naini and Talwani, 1982). Thin lines: line drawing from Fig 5 overlaid.

2006; Collier et al., 2008) did not have this two-fold control to work. So our models are better than the existing ones. Again, we show various volcano-stratigraphic structures on the high quality seismic data and compelling evidences like rift valleys devoid of rift-related sedimentation, axial magma chambers etc. clearly demonstrate that the Laxmi Ridge is unlikely to have a continental sliver beneath the lava pile.

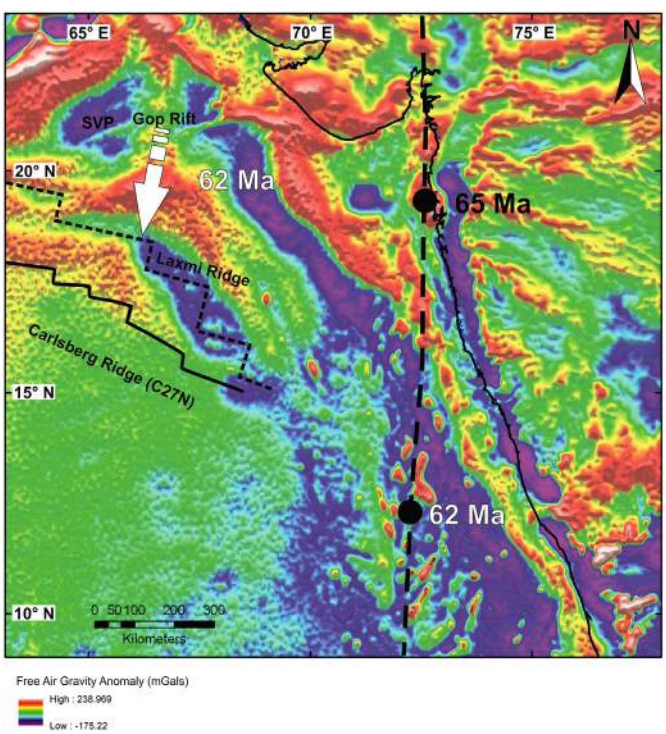

Figure 15. Free air gravity map of the study area with the C27 Carlsberg Ridge (of Royer et al., 2002) and our interpretation of the Laxmi Ridge spreading centre. Ages of the volcanics related to the Réunion hotspot track alongside black dots, 65 Ma: average age of the dated volcanics; 62 Ma: interpolated age between two dated points (Fig. 1 shows the two dated locations). Arrow: Jump of the spreading centre from Gop Rift to the Laxmi Ridge at ~62 Ma.

We identified WSW trending sediment under-filled, narrow, fault-bound rift valleys on the Laxmi Ridge. The following additional arguments show that these rift valleys are not related to continental rifts.

(i) The adjoining rift valleys at Bombay High have ~ 6 km thick sediments (Basu et al., 1980; Roychoudhury and Deshpande, 1982; Gopala Rao, 1990), and in Seychelles it is ~3 km at the NE shelf that is conjugate to this study area (Plummer and Belle, 1995). Rift valleys are expected to host thicker (> 1000 m) sediments. It will be impossible for the terrigenous sediments to avoid every rift valley on a narrow region, now Laxmi Ridge, and fill other rifted grabens on either side, if the Laxmi Ridge were indeed a sliver (as in fig. 1c of Collier et al., 2008).

(ii) A different possibility could be volcanics emplacing on top of an attenuated crust and thereafter the faults in the attenuated crust being reactivated. The problem with this is that the closest magnetic anomaly stripe (C27), indicating a spreading ridge of ~ 61 Ma parallels the rift valleys. Sea floor spreading indicates faulting ended at orthogonally rifted continental margins. So the heat centre due to the spreading ridge would shift temporally away from the faults and the margin. This cannot reactivate those faults. If the magnetic anomaly and the rift valleys were oblique, there faults would reactivate due to the passing-by spreading centre, similar to the Romanche Fracture Zone in the Equatorial Atlantic (e.g. Attoh et al., 2004). Further, an attenuated crust may be considered, where the lower crust is exhumed along a mid-crustal detachment. The thickness of such extended lower crust would be < 5 km (Manatschal, 2004; Whitmarsh and Manatschal, 2012). The total of the crust at the Laxmi Ridge is ~18–22 km (Naini and Talwani, 1982; seismic sections in this study). Considering >8 km thick under-plating, the volcanic cover would be > 7 km over the Laxmi Ridge.

Reactivation of faults crossing this massive volcanic thickness and reaching the top of the ridge is most unlikely, especially after breakup.

(iii) The Laxmi Ridge had been passing through tropical climate zones (Seton et al., 2012's reconstruction) since ~ 65 Ma. Thus, sedimentation is inevitable in the rift valleys if the rift shoulders were near sea surface and stayed in shallow water for some time (~0.5–1 Ma), as expected in continental rift zones. The sediments are Late Paleocene to Recent in the nearby well BRDW-4-1 (location shown in Figs. 3, 10). Thickness of sediments reach a maximum of ~ 500 m in ~ 60 Ma, which means the rate of sedimentation in these valleys was < 10 cm ky^{-1}. This is comparable with deep-water, pelagic sedimentation rates (0.2–10 cm ky^{-1}: Rothwell, 2005; Hüneke and Mulder, 2011). In comparison, continental rift basins have much faster sedimentation rates of 0.2–5 m ky^{-1} (Ravnås and Steel, 1998) and often contain 1000s of m of sediments in grabens of adequate accommodation spaces, e.g. Morley et al. (1999) and Chorowicz (2005) for the East African Rift System and Odinsen et al. (2000) for the North Sea rift. It is possible to have such under-filled rift valleys only if they were formed at abyssal depths i.e. if they were oceanic spreading centres. Total sediment thicknesses at the deepest ocean floor at present day are < 200 m (Divins, 2003; Whittaker et al., 2013). The sedimentation character in rift valleys seen in the SCS profiles resembles pelagic sedimentation in the deep Mid-Atlantic (e.g. Mitchel, 1995; Murdmaa et al., 2012).

The Gop Rift in the Laxmi Basin between the Bombay High and the Laxmi Ridge comprises of a few isolated volcanic mounds over a pre-existing oceanic crust of “normal” thickness. The oceanic crust flexed due to the load of the volcanic mound. These mounds erupted over pre-existing oceanic crust (e.g. pp. 137 of Watts, 2001). Therefore, those mounds possibly are not fossil spreading centres. The thickness of the oceanic crust in such areas matches that of a “normal” oceanic crust: i.e. 7–8 km (Fig. 9).

That the Moho is warped beneath the Laxmi ridge cannot discriminate whether the Laxmi Ridge is of continental—or oceanic crust. We support crustal nature of the Laxmi Ridge to be oceanic rather than continental, and that it is another fossil spreading centre based on the converging evidence of the following arguments.

(i) Deep reflection seismic sections show absence of features expected for continental slivers such as seaward dipping normal faults, prograding sedimentary sequences on flanks etc. The plume related volcanism could overprint such features. But, evidently such features (e.g. normal faults) are imaged on the same data in the landward side, where the centre of volcanism (i.e. along the Réunion hotspot track) was closer to the faults. Also, it is unlikely that they are not imaged in any of the three ion-GXT lines. The degree of volcanism is expected to change along the ridge and the lines are strategically placed to capture the change/segmentation of the ridge. Instead, large SDR sequences often reach (or lie within 2–3 km from) the Moho on the flanks of the ridge (Figs. 7a,b, 8). For continental crust, the SDRs are not expected to be near (within 2–3 km) the Moho (e.g. Jackson et al., 2000), and such deep SDRs (Outer) throughout the Laxmi Ridge is the most important criterion to indicate its volcanic nature.

(ii) Seismic sections constrained by gravity models in this study indicate the crust of the Laxmi Ridge to be of high density. This also matches previous studies such as Pandey et al. (1995), Singh (1999), Rajaram et al. (2011). High density crust may also indicate intruded continental crust, besides oceanic crust. But, combining all the other evidences, the high density also supports the interpretation that Laxmi Ridge is plausibly composed of oceanic crust.

(iii) Fault bound rift valleys with sparse sediments that are not rift related was deciphered in sub-section 4.2. Also, the 110–120° N trends of these rift valleys match with that of the magnetic chron C27 (Figs. 3, 4b-d, 12). Thus, these rifts developed in a deep marine setting i.e. plausibly at a spreading centre, but that was subsequently aborted. This section described in the beginning states that these rift valleys formed possibly at a spreading centre.

(iv) Additionally, the Laxmi Ridge lies presently ~ 4 km deep with almost no sediment at top of the ridge at the SE region. The relief of the Laxmi Ridge in this area is ~ 2–3 km from the surrounding ~ 4–6 km deep oceanic crust. This matches with the global average relief of ~ 2 km (pp. 60 of Frisch et al., 2011) for the mid-oceanic ridges. Abandoned spreading centres, like those in the Mascarene basin do not show the relief because the ridge subsided to the surrounding sea floor. However, plumes near spreading centre supply melts to the latter (Mittelstaedt et al., 2011). Such spreading centres like the Reykjanes Ridge near Iceland mantle plume, the Mid Atlantic Ridge between Ascension and Cape Verde fracture zones influenced by the Ascension mantle plume, have thicker crusts beneath the spreading ridge (e.g. Smallwood and White, 1998; Bruguier et al., 2003; Weir et al., 2001). This enhanced thickness is attributed to higher melting due to the hot mantle plume increasing temperatures by ~ 100 °C at the Moho (Gaherty, 2001; Delorey et al., 2007). The higher temperature lowers densities and increases thermal buoyancy of the asthenosphere. The increased melt and thermal buoyancy uplifts the spreading centre permanently (Höskuldsson et al., 2007). This is more evident in the Reykjanes Ridge in the N Atlantic Ocean, S of Iceland, where the ridge crest lies at < 900 m of bathymetry. The Moho with a characteristic ~ 8 km s^{-1} P-wave velocity lies at > 11 km depth (Smallwood and White, 1998; Chen, 2003; Weir et al., 2001) beneath the ridge crest, decreasing to ~ 6 km away from the ridge. The crust also thins along the ridge farther away from the plume.

The Laxmi Ridge spreading centre was most possibly similar to the Reykjanes Ridge, and the Saurashtra Volcanic Platform (SVP) was equivalent to the present day Iceland island. The Laxmi Ridge spreading centre was plausibly very shallow, merely <1 km deep, and the SVP was exposed sub-aerially (Calvès et al., 2008, 2011; Corfield et al., 2010). The SVP would be an off-track volcanic centre (Fig. 15). The thick crust at the spreading centre thereafter continued subsiding after abandonment and its top reached present day depths of > 4 km. Moho depth measurements reveal that the Laxmi Ridge has a deep crust, formed possibly due to ridge—plume interaction. The ‘root’ of this thick crust prevents the Laxmi Ridge from sinking down to the bathymetries of the surrounding oceanic crust. Note that the relief of the Laxmi Ridge increases from ~ 5 to ~ 3 km towards SE as it came nearer to the plume trail (see Fig. 12a). Lesser subsidence (by ~ 1 km) closer to the Réunion hotspot track is reported to be by convective upwelling of oceanic crust and axis perpendicular flow assisted by the Réunion hotspot during spreading (Ajay and Chaubey, 2008).

(v) We visualized magma chamber(s) beneath the crest of the Laxmi Ridge, similar to many other spreading ridges e.g. Mid Atlantic Ridge (Singh et al., 2006) and Juan de Fuca Ridge

(Canales et al., 2006). See sub-section 3.1.2 for details of axial magma chambers.

(vi) The Carlsberg Ridge of C27 interpreted from magnetic anomalies (from Royer et al., 2002) and the Laxmi Ridge spreading centre interpreted here from seismic- and gravity interpretation in this study match considerably in geometry. The most important outcome is the agreement in the overall trend of the segments, and the individual spreading ridges and fracture zones between the Laxmi- and Carlsberg Ridges.

Enormous volcanism at ~65–60 Ma, surrounding Laxmi Ridge was probably related to the Réunion plume. This is evident from the flexing of the oceanic crust by volcanic mounds aside the ridge (Figs. 8, 9), and also by the voluminous SDRs occurring atop and surrounding the Laxmi Ridge (Figs. 7, 8). The very deep SDRs (see Fig. 8) we observed beneath the Laxmi Ridge on line WC3000 prove that the volcanics continue far underneath the Laxmi Ridge. Therefore, deeper SDRs indicate early volcanism. Continental crustal fragments trapped beneath the huge pile of volcanics are unlikely.

Rangarajan (2006) negated ridge jumps to explain the geometry of the W continental margin of India. The present study disproves this. Rangarajan (2006) considered that Madagascar and Seychelles separated from India coevally (~ 89 Ma). However, subsequent magnetic interpretations (e.g. Collier et al., 2008; Eagles and Hoang, 2014) rebutted his hypothesis. We find that there are two fossil spreading centres in the Laxmi-Gop region, and one more in the Mascarene. Hence, there has to be at least three ridge jumps. The first jump was related to asymmetric spreading in the Mascarene Basin (at 70-65 Ma; Dyment, 1998; Müller et al., 2001; review: Valdiya, 2010). This jump followed the Réunion plume. Spreading anomalies of latest chron C27 are identified in the Mascarene Basin (Bernard and Munschy, 2000). The next two ridges reorganised possibly due to and during Réunion pluming (Fig. 16). The position of the plume at ~ 62 Ma (Figs. 15, 16) possibly aided the jump from Gop Rift to the Laxmi Ridge near chron C27N (~62 Ma) (Minshull et al., 2008; review: Reston and Manatschal, 2011). The position of the plume at 60 Ma (Fig. 1) promoted the jump from Laxmi Ridge to Carlsberg-CIR Ridge at chron C26 (62.5–59.5 Ma) though sea-floor spreading due to the Gop Rift spreading centre possibly continued till ~ 58.5 Ma (Yatheesh et al., 2009; review by Ganerød et al., 2011). There are magnetic anomalies of chron C28 onwards identified in the Laxmi region. Carlsberg-CIR Ridge related spreading started at chron C26 (Fig. 3). Thus, the Seychelles microcontinent separated completely within chrons C28 to C26 (i.e. between 64 and 60 Ma). The separation involved three identifiable ridge reorganizations. The presence and role of asymmetric sea floor spreading remains indeterminate because of the multiple ridge jumps in short magnetic intervals, and undecipherable magnetic anomalies in the Eastern Basin. The plume identifiably triggered the ridge jump. However, whether it is required for the microcontinent separation remains unknown. Though Müller et al. (2001) considered it to be prerequisite for the genesis of micro-continents, subsequent studies show that plume has no role in the separation of microcontinents (e.g. Collier et al., 2008 for Seychelles; Péron-Pinvidic and Manatschal, 2010 for the Jan Mayen). The separation is achieved through multiple re-organizations between competing rift zones. This process is also evident in this area through unsuccessful rifts viz. Gulf of Kutch and Cambay during this period.

Thus, segments of the early-Carlsberg-CIR Ridge appear to be shifting towards the Réunion plume repeatedly, while the W Indian passive margin moved farther away from the plume (Fig. 16). Fragments thus aborted form the present day Gop Rift and the Laxmi Ridge. Such repeat ridge jumps occur at many other terrains

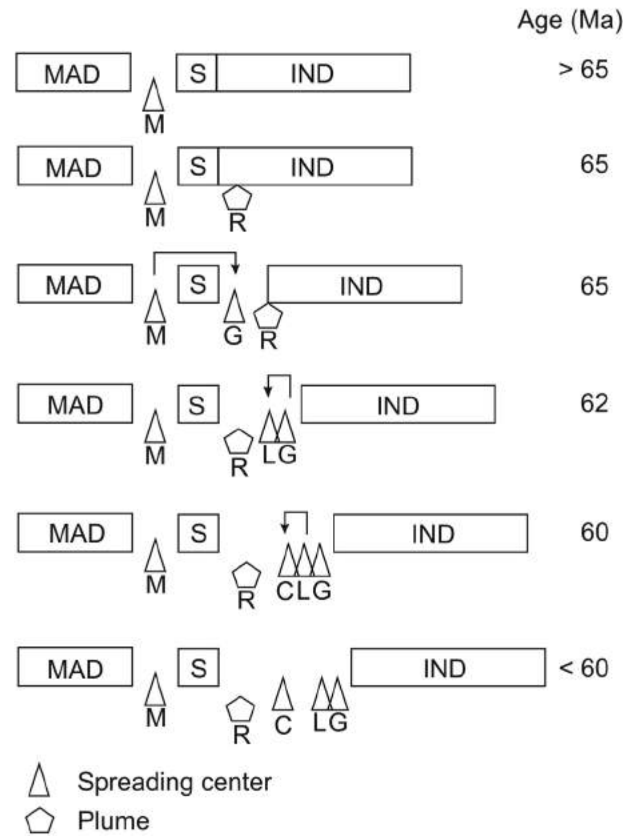

Figure 16. Schematic diagram shows the plate, spreading centre and plume relations for the study area. The spreading centre relocates near the plume repeatedly in geologic time. MAD = Madagascar; S = Seychelles; IND = Indian sub-continent; M = spreading centre in Mascarene basin; G = Gop Rift; L = Laxmi Ridge; C = Carlsberg Ridge; R = Réunion plume. Arrows mark the ridge jumps.

where plumes interact with ridges e.g. at Ascension, Iceland, Walvis, Kerguellen and Galapagos (Martin, 1987; Krishna and Rao, 2000; Barckhausen et al., 2001; Mittelstaedt et al., 2011 and references therein). Time required for ridge jumps depends on (*i*) magmatic heating rate related to the hotspot, (*ii*) spreading rate of the ridge and (*iii*) plate age (Mittelstaedt et al., 2008). Small repeated ridge jumps have been identified in the Pacific (Cande and Haxby, 1991). Dynamic process of magma flux and associated lithospheric heating control recurring ridge jumps (Mittelstaedt et al., 2011). The spreading rates in the Mascarene basin between magnetic chrons C30 to C28 was moderate i.e., 8–12 cm yr^{-1} (Schlich, 1974; Bernard and Munschy, 2000). However, the magmatic heating rate for the Réunion plume was significantly large on a very young oceanic crust. The magnitudes of heating can be ~ 100 °C higher than spreading ridges unaffected by plumes as seen in the Reykjanes Ridge (Gaherty, 2001; Delorey et al., 2007). Because of these favourable factors, ridge jumped rather quickly. There were three jumps between chrons C28 and C26.

6. Conclusions

The Laxmi Ridge is composed of oceanic crust formed at an abandoned oceanic spreading centre. We provide new interpretation of ion-GXT seismic lines by analysing volcanic facies on recently acquired high quality seismic data. Outer and deeper Seaward Dipping Reflectors (SDRs), axial magma chambers, sediment unfilled rift valleys etc. indicate geologically that the Laxmi Ridge is most plausibly a fossilised spreading centre. We combine depths to Moho and other interfaces from Pre-Stack Depth Migrated (PSDM) seismic data and refraction seismic points for 2D forward gravity modelling. We infer the Laxmi Ridge to be composed of high density crust. This strengthens our interpretation that the Laxmi Ridge is of oceanic crustal affinity. Though the debate on the crustal nature of the Laxmi Ridge would still remain owing to the non-uniqueness of geophysical analyses, a better study could be by obtaining drilled core samples from the basement of the Laxmi Ridge for geochemical analyses. The Integrated Ocean Drilling Programme is scheduled to drill the Laxmi Ridge (Exon et al., 2011). If drilled deep enough, such an effort could also generate vital ground truth for Outer SDRs. There were three ridge jumps (Fig. 16) viz. (*i*) spreading in the Mascarene jumped to the Gop Rift, (*ii*) Gop rift: a ~ NW–SE plate movement happened definitely older than chron C28N, which jumped to the Laxmi Ridge; and (*iii*) Laxmi Ridge: a ~ NNE-SSW oriented plate movement of a short duration during chron C28–C27. At this time (~ 63 Ma), Seychelles separated from India forming a microcontinent. The Laxmi Ridge finally jumped to the Carlsberg-CIR Ridge, starting a southward movement of the Seychelles micro-plate at chron C26. This ridge jump is not related to the separation of the microcontinent. The plate movements related to the Gop Rift and the Laxmi Ridge also match the extension directions (~ NW and ~ NNE) deciphered from onland studies in and around Mumbai (= Bombay) region (Bhattacharya et al., 2013; Misra et al., 2014). Though the first ridge jumped due to the spreading asymmetries in the Mascarene Basin, subsequent jumps seems plume assisted. It could be a combination of both but is difficult to comprehend their relative roles due to undecipherable magnetic anomalies (during chron C28 to C26) N and E of the Laxmi Ridge. Spreading asymmetries were identified from chron C26 to C20 on the Carlsberg Ridge (Dyment, 1998). These reorganizations also changed the Seychelles plate movement directions (NW to NNE to N) with each ridge jump. The plume is definitely related to this breakup at ~ 64 Ma. However, its exact role needs further study. Most possibly, the mantle temperature anomaly required for the separation got consumed during the Gop Rift episode (Minshull et al., 2008). Thereafter the Gop spreading centre required the melt flux from the plume to continue the spreading and jumped towards the Laxmi Ridge. Thereafter, when the Indian plate moved away from the plume towards N, the Laxmi Ridge aborted and followed the plume to finally jump to the Carlsberg-CIR Ridge. All the three ridge jumps were rapid and within ~ 64–59 Ma, and definitely followed the plume.

Acknowledgements

AAM and NS thank Reliance Industries Ltd. (Petroleum Exploration) and ion-GXT for the data and permitting publication. AAM and SM acknowledge IIT Bombay's partial financial support. Sudipta Tapan Sinha commented constructively. Discussions with Nishikanta Kundu, Sandipan Saha and Tanmoy Mandal (Reliance Industries Limited), Amit Kumar Sen (IIT Roorkee) and Saibal Gupta (IIT Kharagpur) and were helpful. Sidhartha Bhattacharyya (Alabama University) supplied research papers. We thank Lamont Doherty Earth Observatory for the vintage seismic data rescue project and for providing seismic sections through GeoMappApp (http://www.geomapapp.org). Quick comments on abstract by Hetu Sheth (IIT Bombay), critical internal reviews by W-C Dullo (Geomar) and CH Mehta (IIT Bombay), external thorough review by two anonymous reviewers, and editorial handling by Jonathan Craig, Samuel Chandru and Octavian Catuneanu (Marine and Petroleum Geology) are acknowledged. The Bouguer gravity anomaly data in Figure 12 and Supplementary figures 1, 2, 3 were provided by Fugro-Robertson for Reliance Industries Limited.

Appendix A. Supplementary data

Supplementary data related to this article can be found at http://dx.doi.org/10.1016/j.marpetgeo.2014.08.019.

References

Ajay, K.K., Chaubey, A.K., 2008. Depth anomalies in the Arabian Basin, NW Indian Ocean. Geo-Mar. Lett. 28, 15–22.

Ajay, K.K., Chaubey, A.K., Krishna, K.S., Gopala Rao, D., Sar, D., 2010. Seaward dipping reflectors along the SW continental margin of India: evidence for volcanic passive margin. J. Earth Syst. Sci. 119, 803–813.

Allerton, S., Escartin, J., Searle, R.C., 2000. Extremely asymmetric magmatic accretion of oceanic crust at the ends of slow-spreading ridge segments. Geology 28, 179–182.

Anderson, R.N., Langseth, M.G., Sclater, J.G., 1977. The mechanism of heat transfer through the floor of the Indian Ocean. J. Geophys. Res. 82, 3391–3409.

Armitage, J.J., Collier, J.S., Minshull, T.A., Henstock, T.J., 2011. Thin oceanic crust and flood basalts: India-Seychelles breakup. Geochem. Geophys. Geosyst. 12, Q0AB07.

Arora, B.R., Subba Rao, P.B.V., Nagar, V., 2003. Electrical conductivity signatures of plume-lithosphere interactions in the Indian Ocean. In: Mahadevan, T.M., Arora, B.R., Gupta, K.R. (Eds.), Indian Continental Lithosphere: Emerging Research Trends. Geol. Soc. India, Bangalore, pp. 393–418.

Attoh, K., Brown, L., Guo, J., Heanlein, J., 2004. Seismic stratigraphic record of transpression and uplift on the Romanche transform margin, offshore Ghana. Tectonophysics 378, 1–16.

Barckhausen, U., Ranero, C.R., von Huene, R., Cande, S.C., Roeser, H.A., 2001. Revised tectonic boundaries in the Cocos Plate off Costa Rica: Implications for the segmentation of the convergent margin and for plate tectonic models. J. Geophys. Res. Solid Earth 106, 19207–19220.

Bastia, R., Radhakrishna, M., 2011. Subsurface geology, depositional history, and petroleum systems along the western offshore basins of India. In: Bastia, R., Radhakrishna, M. (Eds.), Developments in Petroleum Science, 59, pp. 269–317.

Basu, D.N., Banerjee, A., Tamhane, D.M., 1980. Source areas and migration trends of oil and gas in Bombay Offshore basin, India. AAPG Bull. 64, 209–220.

Baudot, G., Sapin, F., Ringenbach, J.C., Dall'Asta, M., Lahmi, M., Rojas, H., Davaux, M., 2013. Structuration and subsidence of the French Guyana hyper-oblique margin. In: EAGE/AAPG Workshop on Basin-Margin Wedge Exploration Plays.20–22 November 2013, Lisbon, Portugal.

Bauer, K., Neben, S., Schreckenber, B., Emmermann, R., Hinz, K., Fechner, N., Gohl, K., Schulze, A., Trumbull, R.B., Weber, K., 2000. Deep structure of the Namibia continental margin as derived from integrated geophysical studies. J. Geophys. Res. Solid Earth 105, 25829–25853.

Becker, J.J., Sandwell, D.T., Smith, W.H.F., Braud, J., Binder, B., Depner, J., Fabre, D., Factor, J., Ingalls, S., Kim, S.-H., Ladner, R., Marks, K., Nelson, S., Pharaoh, A., Trimmer, R., Von Rosenberg, J., Wallace, G., Weatherall, P., 2009. Global bathymetry and elevation data at 30 arc seconds Resolution: SRTM30_PLUS. Mar. Geod. 32, 4355–4371.

Bernard, A., Munschy, M., 2000. Were the Mascarene and Laxmi Basins (western Indian Ocean) formed at the same spreading centre? C. R. Acad. Sci. Earth Planet. Sci. 330, 777–783.

Bhattacharya, G.C., Chaubey, A.K., 2001. Western Indian Ocean – a glimpse of the tectonic scenario. In: Sen Gupta, R., Desa, E. (Eds.), The Indian Ocean – a Perspective, vol. 2, pp. 671–731.

Bhattacharya, G.C., Yatheesh, V., 2014. Plate-tectonic evolution of the deep oceanic basins adjoining the western continental margin of India – a proposed model for the early opening scenario. In: Mukherjee, S. (Ed.), Petroleum Geosciences: Indian Contexts. Springer, ISBN 978-3-319-03118-7 (submitted).

Bhattacharya, G.C., Chaubey, A.K., Murty, G.P.S., Srinivas, K., Sarma, K., Subrahmanyam, V., Krishna, K.S., 1994. Evidence for sea-floor spreading in the Laxmi Basin, northeastern Arabian Sea. Earth Planet. Sci. Lett. 125, 211–220.

Bhattacharya, G., Misra, A.A., Bose, N., Mukherjee, S., 2013. Strike-slip brittle shear zone from coastal Deccan in and around Mumbai, India: evidence for N–S extension. In: EGU General Assembly, 7–12 April, Vienna, Austria.

Bhattacharyya, R., Verma, P.K., Majumdar, T.J., 2009. High resolution satellite geoids/gravity over the western Indian offshore for tectonics and hydrocarbon exploration. Indian J. Mar. Sci. 38, 116–125.

Birch, F., 1961. The velocity of compressional waves in rocks to 10 kilobars, Part 2. J. Geophys. Res. 66, 2199–2224.

Biswas, S.K., 1989. Hydrocarbon exploration in western offshore basins of India. In: Recent Geoscientific Studies in the Arabian Sea off India. Geol. Surv. Ind. Sp. Pub. Manipal Power Press, pp. 185–194.

Biswas, S.K., 2012. Status of petroleum exploration in India. Indian Report to the IUGS: 2008–2012. In: Banerjee, D.M., Singhvi, A.K. (Eds.), Glimpse of Geoscience Research in India, Proc. Ind. Sci. Acad, vol. 78, pp. 475–498.

Biswas, S.K., 2014. Active tectonics of western Continental margin of Indo- Pak Craton-Stress source for SCR Earthquakes (in press). J. Earthq. Sci. http://www.joes.org.in/openaccess/P3-Biswas.pdf (accessed of 06.05.14.).

Biswas, S.K., Singh, N.K., 1988. Western Indian Deep-Sea basins: exploration thrust area. ONGC Bull. 25, 1–20.

Biswas, S.K., Thomas, J., 1992. Deccan traps and Indian Ocean volcanism. In: Plummer, P.S. (Ed.), First Indian Ocean Petroleum Seminar: Seychelles. United Nations Department of Technical Co-operation for Development, pp. 187–209.
Borissova, I., Coffin, M.F., Charvis, P., Operto, S., 2003. Structure and development of a micro-continent: Elan Bank in the southern Indian Ocean. Geochem. Geophy. Geosyst. 4, 1071.
Bruguier, N.J., Minshull, T.A., Brozena, J.M., 2003. Morphology and tectonics of the Mid-Atlantic Ridge, 7°–12°S. J. Geophys. Res. Solid Earth 108, 2093.
Calvès, G., Clift, P.D., Inam, A., 2008. Anomalous subsidence on the rifted volcanic margin of Pakistan: no influence from Deccan plume. Earth Planet. Sci. Lett. 272, 231–239.
Calvès, G., Schwab, A.M., Huuse, M., Clift, P.D., Inam, A., 2010. Thermal regime of the northwest Indian margin – comparison with predictions. Mar. Petrol. Geol. 27, 1133–1147.
Calvès, G., Schwab, A.M., Huuse, M., Clift, P.D., Gaina, C., Jolley, D., Tabrez, A.R., Inam, A., 2011. Seismic volcanostratigraphy of the western Indian rifted margin: the pre-Deccan igneous province. J. Geophys. Res. Solid Earth 116, B01101.
Canales, J.P., Singh, S.C., Detrick, R.S., Carbotte, S.M., Harding, A., Kent, G.M., Diebold, J.B., Babcock, J., Nedimović, M.R., 2006. Seismic evidence for variations in axial magma chamber properties along the southern Juan de Fuca Ridge. Earth Planet. Sci. Lett. 246, 353–366.
Cande, S.C., Haxby, W.F., 1991. Eocene propagating rifts in the southwest Pacific and their conjugate features on the Nazca plate. J. Geophys. Res. Solid Earth 96, 19609–19622.
Carmichael, S.M., Akhter, S., Bennett, J.K., Fatimi, M.A., Hosein, K., Jones, R.W., Longacre, M.B., Osborne, M.J., Tozer, R.S.J., 2009. Geology and hydrocarbon potential of the offshore Indus Basin, Pakistan. Petrol. Geosci. 15, 107–116.
Chamoli, A., 2009. Wavelet analysis of geophysical time series. Earth Sci. India 2, 258–275.
Chaubey, A.K., Bhattacharya, G.C., Murty, G.P.S., Srinivas, K., Ramprasad, T., Rao, D.G., 1998. Early Tertiary seafloor spreading magnetic anomalies and paleo- propagators in the northern Arabian Sea. Earth Planet. Sci. Lett. 154, 41–52.
Chen, Y.J., 2003. Influence of the Iceland mantle plume on crustal accretion at the inflated Reykjanes Ridge: magma lens and low hydrothermal activity? J. Geophys. Res. Solid Earth 108, B11.
Chenet, A.L., Quidelleur, Z., Fluteau, F., Courtillot, V., Bajpai, S., 2007. ^{40}K-^{40}Ar dating of the main Deccan large igneous province: further evidence of KTB age and short duration. Earth Planet. Sci. Lett. 263, 1–15.
Chorowicz, J., 2005. The East African rift system. J. Afr. Earth Sci. 43, 379–410.
Christensen, N.I., Mooney, W.D., 1995. Seismic velocity structure and composition of the continental crust: a global review. J. Geophys. Res. Solid Earth 100, 9761–9788.
Clark Jr., S.P., 1966. Handbook of Physical Constants. Geol. Soc. Am. Mem, p. 97.
Clift, P., Gaedicke, C., Edwards, R., Lee, J.I., Hildebrand, P., Amjad, S., White, R.S., Schlüter, H.-U., 2002. The stratigraphic evolution of the Indus Fan and the history of sedimentation in the Arabian Sea. Mar. Geophys. Res. 23, 223–245.
Collier, J.S., Sinha, M.C., 1990. Seismic images of a magma chamber beneath the Lau back-arc spreading centre. Nature 346, 646–648.
Collier, J.S., Sansom, V., Ishizuka, O., Taylor, R.N., Minshull, T.A., Whitmarsh, R.B., 2008. Age of Seychelles–India break-up. Earth Planet Sci. Lett. 272, 264–277.
Corfield, R.I., Carmichael, S., Bennett, J., Akhter, S., Fatimi, M., Craig, T., 2010. Variability in the crustal structure of the West Indian Continental Margin in the Northern Arabian Sea. Petrol. Geosci. 16, 257–265.
Coumes, F., Kolla, V., 1984. Indus Fan: seismic structure, channel migration and sediment thickness in the upper fan. Marine geology and oceanography of Arabian Sea and coastal Pakistan. In: Haq, B.U., Milliman, J.D. (Eds.), Marine geology and Oceanography of the Arabian Sea and Coastal Pakistan, pp. 101–110.
Courtillot, V., Jaupart, C., Manighetti, I., Tapponnier, P., Besse, J., 1999. On causal links between flood basalts and continental breakup. Earth Planet. Sci. Lett. 166, 177–195.
Del Ben, A., Barnaba, C., Taboga, A., 2008. Strike-slip systems as the main tectonic features in the Plio-Quaternary kinematics of the Calabian Arc. Mar. Geophys. Res. 29, 1–12.
Delorey, A.A., Dunn, R.A., Gaherty, J.B., 2007. Surface wave tomography of the upper mantle beneath the Reykjanes Ridge with implications for ridge-hot spot interaction. J. Geophys. Res. Solid Earth 112, B08313.
Detrick, R.S., Buhl, P., Vera, E.E., Mutter, J.C., Madsen, J.A., Brocher, T.M., 1987. Multichannel seismic imaging of a crustal magma chamber along the East Pacific Rise. Nature 326, 35–41.
Divins, D.L., 2003. Total Sediment Thickness of the World's Oceans & Marginal Seas. NOAA National Geophysical Data Center, Boulder, CO.
Duncan, R.A., 1990. The volcanic record of the Rèunion hotspot. In: Duncan, R.A., Backman, J., Peterson, L.C., et al. (Eds.), Proc Ocean Drill Prog, Sci Res, 115, pp. 3–10.
Dyment, J., 1998. Evolution of the Carlsberg Ridge between 60 and 45 Ma— Ridge propagation, spreading asymmetry, and the Deccan-Reunion hotspot. Jour. Geophys. Res. 103, 24067–24084.
Dyment, J., Vadakkeyakath, Y., Bhattacharya, G., 2012. Early opening of Seychelles and India: the gop Basin revisited. In: AGU Fall Meeting, December. Abstracts 1, 5.
Eagles, G., Hoang, H.H., 2014. Cretaceous to present kinematics of the Indian, African and Seychelles plates. Geophys. J. Int. 196, 1–14.
Eagles, G., Wibisono, A.D., 2013. Ridge push, mantle plumes and the speed of the Indian plate. Geophys. J. Int. 194, 670–677.
Elliott, G.M., Berndt, C., Parson, L.M., 2009. The SW African volcanic rifted margin and the initiation of the Walvis Ridge, South Atlantic. Mar. Geophys. Res. 30, 207–214.
Exon, N., Pandey, D., Gallagher, S., Rajan, S., Coffin, M., Takai, K., et al., 2011. Detailed Report on Indian Ocean IODP Workshop Goa, India October 17–18, 2011. http://www.iodp.org/doc_download/3337-a1indianoceaniodpreportfinallowres (accessed on 07.06.14.).
Franke, D., 2013. Rifting, lithosphere breakup and volcanism: comparison of magma-poor and volcanic rifted margins. Mar. Petrol. Geol. 43, 63–87.
Franke, D., Ladage, S., Schnabel, M., Schreckenberger, B., Reichert, C., Hinz, K., Paterlini, M., de Abelleyra, J., Siciliano, M., 2010. Birth of a volcanic margin off Argentina, South Atlantic. Geochem. Geophys. Geosyst. 11, Q0AB04.
Frisch, W., Meschede, M., Blakey, R., 2011. Plate Tectonics: Continental Drift and Mountain Building. Springer, Berlin, pp. 59–69.
Gaherty, J.B., 2001. Seismic evidence for hotspot-induced buoyant flow beneath the Reykjanes Ridge. Science 293, 1645–1647.
Ganerød, M., Torsvik, T.H., Hinsbergen, D.J.J., Van Gaina, C., Corfu, F., Werner, S., Owen-Smith, T.M., Ashwal, L.D., Webb, S.J., Hendriks, B.W.H., 2011. Palaeoposition of the Seychelles microcontinent in relation to the Deccan Traps and the Plume Generation Zone in Late Cretaceous–Early Palaeogene time. In: Hinsbergen, D.J.J., Van, Buiter, S.J.H., Torsvik, T.H., Gaina, C., Webb, S.J. (Eds.), The Formation and Evolution of Africa: a Synopsis of 3.8 Ga of Earth History, Geol. Soc., London, Sp. Pub. 357, pp. 229–252.
Gente, P., Pockalny, R.A., Durand, C., Deplus, C., Maia, M., Ceuleneer, G., Mével, C., Cannat, M., Laverne, C., 1995. Characteristics and evolution of the segmentation of the Mid-Atlantic Ridge between 20°N and 24°N during the last 10 million years. Earth Planet. Sci. Lett. 129, 55–71.
Ghosh, B.N., Zutshi, P.L., 1989. Indian west coast shelf break tectonic features. Geol. Surv. India Sp. Pub 24, 309–318.
Gillis, K.M., 2008. The roof of an axial magma chamber: a hornfelsic heat exchanger. Geology 36, 299–302.
Gillis, K.M., Coogan, L.A., 2002. Anatectic migmatites from the roof of an ocean ridge magma chamber. J. Petrol. 43, 2075–2095.
Goff, J.A., Cochran, J.R., 1996. The Bauer scarp ridge jump: a complex tectonic sequence revealed in satellite altimetry. Earth Planet. Sci. Lett. 141, 21–33.
Gopala Rao, D., 1990. Magnetic studies of basement off the coast of Bombay, west of India. Tectonophysics 175, 317–334.
Green, A., 2011. The late Cretaceous to Holocene sequence stratigraphy of a sheared passive upper continental margin, northern KwaZulu-Natal, South Africa. Mar. Geol. 289, 17–28.
Hall, C.E., Gurnis, M., 2005. Strength of fracture zones from their bathymetric and gravitational evolution. J. Geophys. Res. Solid Earth 110, BO1402.
Hammond, J.O.S., Kendall, J.M., Collier, J.S., Rümpker, G., 2013. The extent of continental crust beneath the Seychelles. Earth Planet. Sci. Lett. 381, 166–176.
Harding, T.P., 1985. Seismic characteristics and identification of negative flower structures, positive flower structures, and positive structural inversion. AAPG Bull. 69, 582–600.
Hopper, J.R., Dahl-Jensen, T., Holbrook, W.S., Larsen, H.C., Lizarralde, D., Korenaga, J., Kent, G.M., Kelemen, P.B., 2003. Structure of the SE Greenland margin from seismic reflection and refraction data: implications for nascent spreading center subsidence and asymmetric crustal accretion during North Atlantic opening. J. Geophys. Res. Solid Earth 108, 2269.
Höskuldsson, Á., Hey, R., Kjartansson, E., Guðmundsson, G.B., 2007. The reykjanes Ridge between 63 10′ N and Iceland. J. Geodyn. 43, 73–86.
Hüneke, H., Mulder, T., 2011. Deep-sea sediments. Dev. Sedimentol. 63, 260–278. Elsevier, New York.
Jackson, M.P.A., Cramez, C., Fonck, J.M., 2000. Role of subaerial volcanic rocks and mantle plumes in creation of South Atlantic margins: implications for salt tectonics and source rocks. Mar. Petrol. Geol. 17, 477–498.
Jacoby, W., Smilde, P.L., 2009. Gravity Interpretation: Fundamentals and Application of Gravity Inversion and Geological Interpretation. Springer-Verlag, Berlin, p. 395.
Karlapati, S., 2004. Seismic Reflection and Bathymetric Study over Deep Offshore Regions off the Central West Coast of India. Ph.D. thesis. University of Goa, p. 180.
Kearey, P., Klepeis, K.A., Vine, F.J., 2009. Global Tectonics, third ed. Wiley-Blackwell, Sussex, p. 130.
Keen, C.A., Dickie, K., Dehler, S.A., 2012. The volcanic margins of the northern Labrador Sea: insights to the rifting process. Tectonics 31, TC1011.
Kodaira, S., Fujie, G., Yamashita, M., Sato, T., Takahashi, T., Takahashi, N., 2014. Seismological evidence of mantle flow driving plate motions at a palaeo-spreading centre. Nat. Geosci. 7, 371–375.
Krishna, K.S., Rao, D.G., 2000. Abandoned Paleocene spreading center in the northeastern Indian Ocean: evidence from magnetic and seismic reflection data. Mar. Geol. 162, 215–224.
Krishna, K.S., Rao, D.G., Sar, D., 2006. Nature of the crust in the Laxmi Basin (14°–20° N), western continental margin of India. Tectonics 25, TC1006.
Levell, B., Argent, J., Doré, A.G., Fraser, S., 2010. Passive margins: overview. In: Vining, B.A., Pickering, S.C. (Eds.), Petroleum Geology: from Mature Basins to New Frontiers – Proceedings of the 7th Petroleum Geology Conference, pp. 823–830.
Lillie, R.J., 1999. Whole Earth Geophysics.an Introductory Textbook for Geologists and Geophysicists. Prentice Hall, Upper Saddle River, pp. 251–277.
Ludwig, J.W., Nafe, J.E., Drake, C.L., 1970. Seismic refraction. In: Maxwell, A.E. (Ed.), The Sea, vol. 4. Wiley, New York, pp. 53–84.

Lunnon, Z.C., White, R.S., Christie, P.A.F., Parkin, C.J., Roberts, A.W., the iSIMM Team, 2005. Seaward dipping reflectors across the northeast Faroes volcanic margin. EGU Geophys. Res. Abstr. 7, 01549.
MacLeod, C.J., Yaouancq, C., 2000. A fossil melt lens in the Oman ophiolite: implications for magma chamber processes at fast spreading ridges. Earth Planet. Sci. Lett. 176, 357–373.
Mahadevan, T.M., 1994. Deep Continental structures of India: a review. Geological Society of India, Bangalore, pp. 411–438.
Mahoney, J.J., 1988. Deccan traps. In: MacDougall, J.D. (Ed.), Continental Flood Basalts. Kluwer, Dordrecht, pp. 151–194.
Manatschal, G., 2004. New models for evolution of magma-poor rifted margins based on a review of data and concepts from West Iberia and the Alps. Int. J. Earth Sci. 93, 432–466.
Manatschal, G., Karner, G.D., 2012. Inter-relationship between the tectonic and magmatic evolution of hyper-extended margins and break-up. Geophys. Res. Abstr. 14. EGU2012–3886, 2012, EGU General Assembly 2012.
Martin, A.K., 1987. Plate reorganisations around Southern Africa, hot-spots and extinctions. Tectonophysics 142, 309–316.
Maus, S., Sazonova, T., Hemant, K., Fairhead, J.D., Ravat, D., 2007. National geophysical data Center candidate for the world digital magnetic anomaly map. Geochem. Geophys. Geosyst. 8, Q06017.
McKenzie, D., 1978. Some remarks on the development of sedimentary basins. Earth Planet. Sci. Lett. 40, 25–32.
Menzies, M.A., Klemperer, S.L., Ebinger, C.J., Baker, J., 2002. Characteristics of volcanic rifted margins. In: Menzies, M.A., Klemperer, S.L., Ebinger, C.J., Baker, J. (Eds.), Volcanic Rifted MarginsGeol. Soc. Am. Spec. Pap. 362, pp. 1–14.
Mignot, A., Mauffret, A., 1986. Seismic stratigraphy of the Neogene Sequence at Site 587. Deep Sea Drill. Proj. Proc. 90, 1339–1344.
Miles, P.R., Munschy, M., Segoufin, J., 1998. Structure and early evolution of the Arabian Sea and East Somali Basin. Geophys. J. Int. 134, 876–888.
Minshull, T.A., Lane, C.I., Collier, J.S., Whitmarsh, R.B., 2008. The relationship between rifting and magmatism in the northeastern Arabian Sea. Nat. Geosci. 1, 463–467.
Mishra, D.C., 2012. Gravity and Magnetic Methods in Geological Studies: Principles, Integrated Exploration and Plate Tectonics. B.S. Publications, Hyderabad, pp. 329–372.
Misra, A.A., Mukherjee, S., 2014. Role of Tectonic Inheritance in Rifting and Passive Margin Architecture (in preparation).
Misra, A.A., Sinha, S.T., Srivastava, D.C., Choudhuri, M., 2009. Photo of the month: positive flower structure in the Archean granite gneiss of southern India. India. J. Struct. Geol. 31, 545.
Misra, A.A., Bhattacharya, G., Mukherjee, S., Bose, N., 2014. Near N-S paleo-extension in the western Deccan region in India: does it link strike-slip tectonics with India-Seychelles rifting? Int. J. Earth Sci. 103, 1645–1680.
Mitchel, N.C., 1995. Diffusion transport model for pelagic sediments on the Mid-Atlantic Ridge. J. Geophys. Res. 100, 19991–20009.
Mittelstaedt, E., Ito, G., Behn, M.D., 2008. Mid-ocean ridge jumps associated with hotspot magmatism. Earth Planet. Sci. Lett. 266, 256–270.
Mittelstaedt, E., Ito, G., van Hunen, J., 2011. Repeat ridge jumps associated with plume-ridge interaction, melt transport, and ridge migration. J. Geophys. Res. 116, B01102.
Morgan, J.P., Ghen, Y.J., 1993. Dependence of ridge-axis morphology on magma supply and spreading rate. Nature 364, 706–708.
Morley, C.K., Ngenoh, D.K., Ego, J.K., 1999. Introduction to the east african rift system. In: Morley, C.K. (Ed.), Geoscience of Rift Systems – Evolution of East Africa, AAPG Studies in Geology, vol. 44, pp. 1–18.
Morley, C.K., Smith, M., Carter, A., Charusiri, P., Chantraprasert, S., 2007. Evolution of deformation styles at a major restraining bend, constraints from cooling histories, Mae Ping fault zone, western Thailand. In: Cunningham, W.D., Mann, P. (Eds.), Tectonics of Strike-slip Restraining and Releasing Bends, Geol. Soc., London, Sp. Pub. 290, pp. 325–349.
Mukherjee, S., 2013. Deformation Microstructures in Rocks. Springer.
Mukherjee, S., 2014a. Atlas of Shear Zone Structures in Meso-scale. Springer.
Mukherjee, S., 2014b. Review of flanking structures in meso- and micro-scales. Geol. Mag. http://dx.doi.org/10.1017/S0016756813001088 (in press).
Mukherjee, S., Koyi, H.A., 2009. Flanking microstructures. Geol. Mag. 146, 517–527.
Mukhopadhyay, R., Ghosh, A.K., Iyer, S.D., 2008. The Indian Ocean nodule field – geology and resource potential. In: Hale, M. (Ed.), Handbook of Exploration and Environmental Geochemistry, vol. 9. Elsevier, Amsterdam, p. 34.
Müller, R.D., Gaina, C., Roest, W., Hansen, D.L., 2001. A recipe for microcontinent formation. Geology 29, 203–206.
Murdmaa, I.O., Levchenko, O.V., Marinova, J.G., 2012. Quaternary seismic facies of the Atlantic Continental Rise. Lithol. Mineral Resour. 47, 379–400.
Mutter, J.C., Carbotte, S.M., Su, W.S., Xu, L., Bhul, P., Detrick, R.S., Kent, G.M., Orcutt, J.A., Harding, A.J., 1995. Seismic images of active magma systems beneath the East Pacific rise between 17°05′ and 17°35′ S. Science 268, 391–395.
Nafe, J.F., Drake, C.L., 1957. Variation with depth in shallow and water marine sediments of porosity, density and the velocities of compressional and shear waves. Geophysics 12, 43–56.
Naini, B.R., Talwani, M., 1982. Structural framework and the evolutionary history of the continental margin of western India. In: Watkins, J.S., Drake, C.L. (Eds.), Studies in Continental Margin Geology, Am. As. Petrol. Geol., Memoir, vol. 34, pp. 167–191.
Nair, N., Anand, S.P., Rajaram, M., 2013. Tectonic framework of laccadive Ridge in western Continental margin of India. Mar. Geol. 346, 79–90.
NELP VII, 2007. Mumbai Offshore Basin Document (accessed 31.08.13.). http://www.infraline.com/ong/upstream/nelp-vii/mumbai-offshore_basin_nelp_vii.pdf.
Nemčok, M., Sinha, S.T., Stuart, C.J., Welker, C., Choudhuri, M., Sharma, S.P., Misra, A.A., Sinha, N., Venkatraman, S., 2013. East Indian margin evolution and crustal architecture: integration of deep reflection seismic interpretation and gravity modeling. In: Mohriak, W.U., Danforth, Al, Post, P.J., Brown, D.E., Tari, G.T., Nemčok, M., Sinha, S.T. (Eds.), Conjugate Divergent Margins, Geol. Soc., London, Sp. Pub. 369, pp. 477–496.
Odinsen, T., Reemst, P., Van Der Beek, P., Faleide, J.I., Gabrielsen, R.H., 2000. Permo-Triassic and Jurassic extension in the northern North Sea: results from tectonostratigraphic forward modelling. In: Nøttvedt, A. (Ed.), Dynamics of the Norwegian Margin, Geol. Soc., London, Sp. Pub. 167, pp. 83–103.
Owen-Smith, T.M., Ashwal, L.D., Torsvik, T.H., Ganerød, M., Nebel, O., Webb, S.J., Werner, S.C., 2013. Seychelles alkaline suite records the culmination of Deccan Traps continental flood volcanism. Lithos 182, 33–47.
Pandey, O.P., Agrawal, P.K., Negi, J.G., 1995. Lithospheric structure beneath Laxmi Ridge and late Cretaceous geodynamic events. Geo-Mar. Lett. 15, 85–91.
Péron-Pinvidic, G., Manatschal, G., 2010. From microcontinents to extensional allochthons: witnesses of how continents break apart? Petrol. Geosci. 16, 189–197.
Péron-Pinvidic, G., Manatschal, G., Gernigon, L., Gaina, G., 2010. The formation and evolution of crustal blocks at rifted margins: new insights from the interpretation of the Jan Mayen microcontinent. In: Central & North Atlantic Conjugate Margins Conference, Lisbon, vols. 231–235. http://metododirecto.pt/CM2010/index.php/vol/article/view/105 (accessed 17.09.13.).
Planke, S., Alvestad, E., 1999. Seismic volcanostratigraphy of the extrusive breakup complexes in the northeast atlantic: implications from ODP/DSDP drilling. In: Larsen, H.C., Duncan, R.A., Allan, J.F., Brooks, K. (Eds.), Proc. Ocean Dril. Prog., Sci. Res., vol. 163, pp. 3–16.
Planke, S., Eldholm, O., 1994. Seismic response and construction of seaward dipping wedges of flood basalts: Vøring volcanic margin. J. Geophys. Res. Solid Earth 99, 9263–9278.
Planke, S., Alvestad, E., Eldholm, O., 1999. Seismic characteristics of basaltic extrusive and intrusive rocks. Lead. Edge 18, 342–348.
Planke, S., Symonds, P.A., Alvestad, E., Skogseid, J., 2000. Seismic volcanostratigraphy of large-volume basaltic extrusive complexes on rifted margins. J. Geophys. Res. Solid Earth 105, 19335–19351.
Plummer, PhS., Belle, E.R., 1995. Mesozoic tectono-stratigraphic evolution of the Seychelles microcontinent. Sedi. Geol. 96, 73–91.
Plummer, PhS., Joseph, P.R., Samson, P.J., 1998. Depositional environments and oil potential of Jurassic/Cretaceous source rocks within the Seychelles microcontinent. Mar. Petrol. Geol. 15, 385–401.
Prodehl, C., Mooney, W.D., 2012. Exploring the Earth's crust: history and results of controlled-source seismology. Geol. Soc. Am. Mem. 208, 685.
Radha Krishna, M., Verma, R.K., Purushotham, A.K., 2002. Lithospheric structure below the eastern Arabian Sea and adjoining West Coast of India based on integrated analysis of gravity and seismic data. Mar. Geophys. Res. 23, 25–42.
Rajaram, M., Anand, S.P., Majumdar, T.J., 2011. Structure and tectonics of the Indian offshore region from satellite-derived geopotential data. In: Proceedings of the Second Swarm International Science Meeting Held at GFZ, Potsdam, Germany, vol. 24. http://www.congrex.nl/09C24/S2_Posters/S2_P01_Rajaram_paper.pdf (accessed 22.04.11.).
Rangarajan, S., 2006. Did Madagascar and Seychelles separate Simultaneously from India?. In: 6th International Conference & Exposition on Petroleum Geophysics, Kolkata. http://www.spgindia.org/conference/6thconf_kolkata06/124.pdf (accessed 07.06.14.).
Ravnås, R., Steel, R.J., 1998. Architecture of Marine Rift-Basin Successions. AAPG Bull. 82, 110–146.
Reeves, C., 2013. The global tectonics of the Indian Ocean and its relevance to India's western margin. J. Geophys. 34, 87–94.
Reeves, C., 2014. The position of Madagascar within Gondwana and its movements during Gondwana dispersal. J. Afr. Earth Sci. 94, 45–57.
Reeves, C., de Wit, M., 2000. Making ends meet in Gondwana: retracing the transforms of the Indian Ocean and reconnecting continental shear zones. Terra Nova 12, 272–280.
Reston, T., Manatschal, G., 2011. Rifted margins: building blocks of later collision. In: Brown, D., Ryan, P.D. (Eds.), Arc-continent Collision. Springer, Berlin, pp. 3–22.
Rey, S.S., Eldholm, O., Planke, S., 2003. Formation of the jan mayen microcontinent, the Norwegian Sea. In: American Geophysical Union, Fall Meeting 2003 abstract #T31D-0872.
Rosendahl, B.R., Meyers, J., Groschel, H., Scott, D., 1992. Nature of the transition from continental to oceanic crust and the meaning of reflection Moho. Geology 20, 721–724.
Rothwell, R.G., 2005. Deep ocean pelagic oozes. In: Selley, R.C., McCocks, L.R., Plimer, I.R. (Eds.), Encyclopedia of Geology, vol. 5. Elsevier Ltd., Oxford, p. 77.
Rothwell, R.G., Alibés, B., Weaver, P.P.E., 1998. Seismic facies of the Madeira Abyssal Plain: a correlation between seismic reflection profile and borehole data. In: Weaver, P.P.E., Schmincke, H.-U., Firth, J.V., Duffield, W. (Eds.), Proc. Ocean Drill. Prog., Sci. Res., vol. 157, pp. 473–498.
Roychoudhury, S.C., Deshpande, S.V., 1982. Regional distribution of carbonate facies, Bombay offshore region, India. AAPG Bull. 66, 1483–1496.
Royer, J.-Y., Chaubey, A.K., Dyment, J., Bhattacharya, G.C., Srinivas, K., Yatheesh, V., Ramprasad, T., 2002. Paleogene plate tectonic evolution of the Arabian and Eastern Somali basins. In: Clift, P.D., Kroon, D., Gaedicke, C., Craig, J. (Eds.), The

Tectonic and Climatic Evolution of the Arabian Sea Region, Geol. Soc. London, Spec. Pub. 195, pp. 7–23.
Rudnick, R.L., Fountain, D.M., 1995. Nature and composition of the continental crust: a lower crustal perspective. Rev. Geophys. 33, 267–309.
Samal, J.K., Dwivedy, R.N., Mayor, S., 2011. Magmatic seismo-facies and crustal architecture along selected profiles in Arabian Sea, West Coast of India. In: The 2nd South Asian Geoscience Conference and Exhibition, GEOIndia 2011, 12–14th Jan, 2011,Gearter Noida, New Delhi, India- Extended Abstract. http://www.searchanddiscovery.com/pdfz/documents/2012/50743samal/ndx_samal.pdf.html (accessed 07.06.14.).
Sandwell, D.T., Smith, W.H.F., 2009. Global marine gravity from retracked Geosat and ERS-1 altimetry: ridge Segmentation versus spreading rate. J. Geophys. Res. 114, B01411.
Schlich, R., 1974. Sea floor spreading history and deep sea drilling results in the Madagascar and Mascarene basins, Western Indian Ocean. Deep Sea Drill. Project-Reports Publ. 25, 663–678.
Schlüter, T., 2006. Geological Atlas of Africa. Springer, New York, pp. 216–219.
Scott, R.A., Lucy, A.R., Jones, S.M., Sinclair, S., Pickles, C.S., 2005. Development of the Jan Mayen microcontinent by linked propagation and retreat of spreading ridges. In: Wandas, B.T.G., Nystuen, J.P., Eide, E.A., Gradstein, F.M. (Eds.), Onshore-offshore Relationships on the North Atlantic Margin, vol. 12. Norway Petroleum Society (NPF) Sp. Pub, pp. 69–82.
Searle, R., 2013. Mid-ocean Ridges. Cambridge University Press, New York, p. 318.
Seton, M., Müller, R., Zahirovic, S., Gainab, C., Torsvik, T., Shephard, G., Talsmaa, A., Gurnis, M., Turner, M., Maus, S., Chandler, M., 2012. Global continental and ocean basin reconstructions since 200 Ma. Earth-Sci. Rev. 113, 212–270.
Singh, A.P., 1999. The deep crustal accretion beneath the Laxmi Ridge in the northeastern Arabian Sea: the plume model again. J. Geodyn. 27, 609–622.
Singh, A.P., 2002. Impact of Deccan volcanism on deep crustal structure along western part of Indian mainland and adjoining Arabian Sea. Curr. Sci. 82, 316–325.
Singh, S.C., 2011. Crustal reflectivity (oceanic) and magma Chamber. In: Gupta, H.K. (Ed.), Encyclopedia of Solid Earth Geophysics. Dordrecht, The Netherlands, pp. 78–89.
Singh, A.P., Mall, D.M., 1998. Crustal accretion beneath Koyana coastal region (India) and late Cretaceous geodynamics. Tectonophysics 290, 285–297.
Singh, S.C., Crawford, W.C., Carton, H., Seher, T., Combier, V., Cannat, M., Canales, J.P., Düsünür, D., Escartin, J., Miranda, J.M., 2006. Discovery of a magma chamber and faults beneath a Mid-Atlantic Ridge hydrothermal field. Nature-Lett. 442, 1029–1032.
Smallwood, J.R., White, R.S., 1998. Crustal accretion at the Reykjanes Ridge, 61°–62° N. J. Geophys. Res. Solid Earth 103, 5185–5201.
Standish, J.J., Sims, K.W., 2010. Young off-axis volcanism along the ultraslow-spreading Southwest Indian Ridge. Nat. Geosci. 3, 286–292.
Stein, C.A., Stein, S., 1992. A model for the global variation in oceanic depth and heat flow with lithospheric age. Nature 359, 123–129.
Subrahmanyam, C., Chand, S., 2006. Evolution of the passive continental margins of India—a geophysical appraisal. Gond. Res. 10, 167–178.
Symonds, P.A., Planke, S., Frey, O., Skogseid, J., 1998. Volcanic evolution of the Western Australian continental margin and its implications for basin development. In: Purcell, P.G., Purcell, R.R. (Eds.), The Sedimentary Basins of Western Australia. Pet. Explor. Soc, Australia. Perth, Australia, pp. 33–54.
Talwani, M., Reif, C., 1998. Laxmi Ridge – a continental sliver in the Arabian Sea. Mar. Geophys. Res. 20, 259–271.
Todal, A., Edholm, O., 1998. Continental margin off Western India and Deccan large igneous province. Mar. Geophys. Res. 20, 273–291.
Torsvik, T.H., Amundsen, H.E., Hartz, H., Corfu, F., Kusznir, N., Gaina, C., Doubrovine, P.V., Steinberger, B., Ashwal, L.D., Jamtveit, B., 2013. A Precambrian microcontinent in the Indian Ocean. Nat. Geosci. 6, 223–227.
Touloukian, Y.S., Judd, W.R., Roy, R.F., 1981. Physical Properties of Rocks and Minerals. McGraw-Hill, New York, pp. 230–411.
Vaidyanadhan, R., Ramakrishnan, M., 2008. Geology of India, vol. 2. Geological Society of India, Bangalore, pp. 907–932.
Valdiya, K.S., 2010. The Making of India: Geodynamic Evolution. McMillan Publishing India Ltd, Delhi, p. 634.
Watts, A.B., 2001. Isostasy and Flexure of the Lithosphere. Cambridge University Press, Cambridge, UK, p. 137, 360–366.
Weir, N.R., White, R.S., Brandsdóttir, B., Einarsson, P., Shimamura, H., Shiobara, H., 2001. Crustal structure of the northern Reykjanes Ridge and Reykjanes Peninsula, southwest Iceland. J. Geophys. Res. Solid Earth 106, 6347–6368.
Whiting, B.M., Karner, G.D., Driscoll, N.W., 1994. Flexural and stratigraphic development of the west Indian continental margin. J. Geophys. Res. 99, 13791–13811.
Whitmarsh, R.B., Manatschal, G., 2012. Evolution of magma poor continental margins: from rifting to the onset of seafloor spreading. In: Phanerozoic Passive Margins, Cratonic Basins and Global Tectonic Maps 1c, pp. 303–317.
Whittaker, J., Goncharov, A., Williams, S., Müller, R.D., Leitchenkov, G., 2013. Global sediment thickness data set updated for the Australian-Antarctic Southern Ocean. Geochem. Geophys. Geosyst. 14, 3297–3305.
Yatheesh, V., Bhattacharya, G.C., Dyment, J., 2009. Early oceanic opening off western India-Pakistan margin: the gop Basin revisited. Earth Planet. Sci. Lett. 284, 399–408.
Yatheesh, V., Dyment, J., Bhattacharya, G.C., Muller, R.D., 2013. Deciphering detailed plate kinematics of the Indian Ocean and developing a unified model for east Gondwanaland reconstruction: an Indian Australian- French initiative. DCS-DST News January 2013 2–9.
Zou, C., 2013. Volcanic Reservoirs in Petroleum Exploration. Petroleum Industry Press, Elsevier, Waltham, p. 4.